Parameter Estimation for Mechanical Systems Using an Extended Kalman Filter

Emmanuel D. Blanchard (eblancha@vt.edu)

Advanced Vehicle Dynamics Lab

Center for Vehicle Systems and Safety, Virginia Tech, Blacksburg, VA 24061– 0238

Adrian Sandu (sandu@cs.vt.edu)

Computer Science Department and the Center for Vehicle Systems and Safety

Virginia Tech, Blacksburg, VA 24061

Corina Sandu (csandu@vt.edu)

Advanced Vehicle Dynamics Lab

Center for Vehicle Systems and Safety, Virginia Tech, Blacksburg, VA 24061– 0238

Abstract

This paper proposes a new computational approach based on the Extended Kalman Filter (EKF) in order to apply the polynomial chaos theory to the problem of parameter estimation, using direct stochastic collocation. The Kalman filter formula is used at each time step in order to update the polynomial chaos of the uncertain states and the uncertain parameters. The main advantage of this method is that the estimation comes in the form of a probability density function rather than a deterministic value, combined with the fact that simulations using polynomial chaos methods are much faster than Monte Carlo simulations. The proposed method is applied to a nonlinear four degree of freedom roll plane model of a vehicle, in which an uncertain mass with an uncertain position is added on the roll bar. A major drawback was identified: the EKF can diverge when using a high sampling frequency, which might prevent the use of enough data to obtain accurate results when a low sampling frequency is necessary. When applying the polynomial chaos theory to the EKF, numerical errors can accumulate even faster than in the general case due to the truncation in the polynomial chaos expansions, which is illustrated on a simple example. An alternative EKF approach which consists of applying the filter formula on all the observations at once usually yields better results, but can still sometimes fail to produce very accurate results. Therefore, using different sampling rates in order to verify the coherence of the results and comparing the results to a different approach is strongly recommended.

Keywords - Parameter Estimation, Polynomial Chaos, Collocation, Halton/Hammersley Algorithm, Extended Kalman Filter (EKF), Vehicle Dynamics

1. Introduction and background

The polynomial chaos theory has been shown to be consistently more efficient than Monte Carlo simulations in order to assess uncertainties in mechanical systems (Sandu *et al.*, 2006a–2006b). This paper extends the polynomial chaos theory to the problem of parameter estimation, and illustrates it on a nonlinear four degree of freedom roll plane model of a vehicle, in which an uncertain mass with an uncertain position is added on the roll bar.

Parameter estimation is an important problem, because many parameters simply cannot be measured physically with good accuracy, especially in real time applications. The method presented in this paper has the advantage of being able to deal with non-Gaussian parametric uncertainties. Parameter estimation is also a very difficult problem, especially for large systems, and a lot of effort devoted to it would be needed. Estimating a large number of parameters often proved to be computationally too expensive. This has led to the development of techniques determining which parameters affect the system's dynamics the most, in order to choose the parameters that are important to estimate (Sohns *et al.*, 2006). Sohns *et al.* (2006) proposed the use of activity analysis as an alternative to sensitivity-based and principal component-based techniques. Their approach combines the advantages of the sensitivity-based techniques (i.e., being efficient for large models) and the component-based techniques (i.e., keeping parameters that can be physically interpreted). Zhang and Lu (2004) combined the Karhunen–Loeve decomposition and perturbation methods with polynomial expansions in order to evaluate higher-order moments for saturated flow in randomly heterogeneous porous media.

The polynomial chaos method started to gain attraction after Ghanem and Spanos (1990, 1991, 1993, 2003) applied it successfully to the study of uncertainties in structural mechanics and vibration using Wiener-Hermite polynomials. Xiu extended the approach to general formulations based on Wiener-Askey polynomials family (Xiu and Karniadakis, 2002a), and applied it to fluid mechanics (Xiu *et al.*, 2002; Xiu and Karniadakis, 2002b, 2003). Sandu *et al.* applied for the first time the polynomial chaos method to multibody dynamic systems (Sandu *et al.* 2004, 2005, 2006a, 2006b), terramechanics (Li *et al.*, 2005; Sandu *et al.*, 2006c), and parameter estimation (Blanchard *et al.*, 2007a - 2007b).

The fundamental idea of polynomial chaos approach is that random processes of interest can be approximated by sums of orthogonal polynomial chaoses of random independent variables. In this context, any uncertain parameter can be viewed as a second order random process (processes with finite variance; from a physical point of view they have finite energy). Thus, a second order random process $X(\vartheta)$, viewed as a function of the random event ϑ, can be expanded in terms of orthogonal polynomial chaos (Ghanem and Spanos, 2003) as:

$$X(\vartheta) = \sum_{j=1}^{\infty} c^j \psi^j(\xi(\vartheta)) \tag{1}$$

Here $\psi^j(\xi_{i_1} \cdots \xi_{i_n})$ are generalized Askey-Wiener polynomial chaoses, in terms of the multi-dimensional random variable $\xi = (\xi_{i_1} \cdots \xi_{i_n})$. The Askey-Wiener polynomial chaoses form a basis. The multi-dimensional basis functions are tensor products of 1-dimensional polynomial basis:

$$\psi^j(\xi_1 \cdots \xi_n) = \prod_{k=1}^{n} P_k^{l_k}(\xi_k), \; j = 1, 2, \cdots, S; \; l_k = 1, 2, \cdots, p \tag{2}$$

where $S = \dfrac{(n+p)!}{n!\,p!}$, n is the number of random variables ξ, and p is the maximum order of the polynomial basis. The total number of terms increases rapidly with n and p.

The basis functions are selected depending on the type of random variable functions. For Gaussian random variables the basis functions are Hermite polynomials, for uniformly distributed random variables the basis functions are Legendre polynomials, for beta distributed random variables the basis functions are Jacobi polynomials, and for gamma distributed random variables the basis functions are Laguerre polynomials (Xiu and Karniadakis, 2002a, 2003). In practice, a truncated expansion of equation (1) is used,

$$X = \sum_{j=1}^{S} c^j \psi^j(\xi) \tag{3}$$

In the deterministic case, a second order unconstrained system can be described by the following Ordinary Differential Equation (ODE):

$$\begin{cases} \dot{x} = v \\ \dot{v} = f(x,v) \\ x(t_0) = x_0 \\ v(t_0) = v_0 \end{cases} \tag{4}$$

In the stochastic framework developed in this study, the displacement $x(t)$, the velocity $v(t)$, and the set of parameters $\theta \in \Re^{n_P}$ (the set of n_P parameters being possibly uncertain) of a second order unconstrained system can be expanded using equation (3) as:

$$x_m(t,\xi) = \sum_{i=1}^{S} x_m^i(t)\psi^i(\xi), \quad v_m(t,\xi) = \sum_{i=1}^{S} v_m^i(t)\psi^i(\xi), \quad \theta_m(\xi) = \sum_{i=1}^{S} \theta_m^i \psi^i(\xi) \tag{5}$$

Propagating equation (5) through the deterministic system of equations of the system, one obtains:

$$\begin{cases} \dot{x}_{m,k}^i = v_{m,k}^i \\ \sum_{i=1}^{S} \dot{v}_{m,k}^i \, \psi^i(\xi) = F_k(t, \sum_{j=1}^{S} x_m^j \, \psi^j(\xi), \sum_{j=1}^{S} v_m^j \, \psi^j(\xi); \sum_{j=1}^{S} \theta_m^j \, \psi^j(\xi)) \\ x_m(t_0) = x_{m,0}, \;\; t_0 \le t \le t_F \end{cases} \tag{6}$$

To derive evolution equations for the stochastic coefficients $x_m^i(t)$ we impose that equation (6) holds at a given set of collocation vectors $\mu^i = \left[\mu_1^i \;\cdots\; \mu_d^i\right]^T$ for all $1 \le i \le S$. This leads to:

$$\dot{x}_m^i = v_m^i, \;\; \sum_{i,j=1}^{S} A_{i,j} \, \dot{v}_m^j = F\left(t, \sum_{m=1}^{S} A_{i,m} \, x_m^m, \sum_{m=1}^{S} A_{i,m} \, v_m^m; \sum_{m=1}^{S} A_{i,m} \, \theta_m^m\right) \tag{7}$$

where A represents the matrix of basis function values at the collocation points:

$$A = \left(A_{i,j}\right), \;\; A_{i,j} = \psi^j(\mu^i), \;\; 1 \le i \le S, \;\; 1 \le j \le S \tag{8}$$

The collocation points have to be chosen such that A is nonsingular. The collocation system can be written as:

$$\dot{X}^i = V^i, \;\; \dot{V}^i = F\left(t, X^i, V^i, \Theta^i\right), \;\; 1 \le i \le S \tag{9}$$

After integration, the stochastic solution coefficients are recovered using:

$$x^i(t) = \sum_{j=1}^{S} \left(A^{-1}\right)_{i,j} \, X^j(t), \;\; v^i(t) = \sum_{j=1}^{S} \left(A^{-1}\right)_{i,j} \, V^j(t) \tag{10}$$

The mean values of $x(t)$ and $v(t)$ are $x^1(t)\psi^1(\xi)$ and $v^1(t)\psi^1(\xi)$, respectively.

The standard deviations of $x(t)$ and $v(t)$ are given by:

$$\sqrt{\int_\Omega \left(\sum_{i=2}^{S} x^i(t)\psi^i(\xi)\right)^2 \rho(\xi) d\xi}, \;\; \sqrt{\int_\Omega \left(\sum_{i=2}^{S} v^i(t)\psi^i(\xi)\right)^2 \rho(\xi) d\xi} \tag{11}$$

where is Ω is the space of possible value for the unknown variables and where $\rho(\xi)$ is the probability distribution of the multi-dimensional random variable $\xi = (\xi_{i_1} \cdots \xi_{i_n})$.

When the basis functions are orthogonal polynomials, the standard deviations of $x(t)$ and $v(t)$ are given by:

$$\sum_{i=2}^{S} \left(x^i(t)\right)^2 \sqrt{\int_\Omega <\psi^i(\xi), \psi^i(\xi)> d\xi}, \;\; \sum_{i=2}^{S} \left(v^i(t)\right)^2 \sqrt{\int_\Omega <\psi^i(\xi), \psi^i(\xi)> d\xi} \tag{12}$$

When the basis are orthonormal, the standard deviations of $x(t)$ and $v(t)$ are given by:

$$\sum_{i=2}^{S}\left(x^i(t)\right),\ \sum_{i=2}^{S}\left(v^i(t)\right) \tag{13}$$

The Probability Density Functions (PDF) of $x(t)$ and $v(t)$ are obtained by drawing histograms of their values using a Monte Carlo simulation and normalizing the area under the curves obtained. This is not computationally expensive since the Monte Carlo simulation is run on the final result, and not for the whole process. For instance, the ODE is run the same number of times as the number of collocation points, which is typically much lower than the number of runs used for the Monte Carlo simulation.

2. Extended Kalman Filter approach for parameter estimation

Optimal parameter estimation combines information from three different sources: the physical laws of evolution (encapsulated in the model), the reality (as captured by the observations), and the current best estimate of the parameters. The information from each source is imperfect and has associated errors. Consider the mechanical system model (6) which advances the state in time represented in a simpler notation:

$$y_k = \begin{bmatrix} x_k \\ v_k \\ \theta_k \end{bmatrix},\quad y_k = M\left(t_{k-1}, y_{k-1}\right),\quad y_0 = y\left(t_0\right),\quad k = 1, 2, \ldots, N \tag{14}$$

The state of the model $y_k \in \Re^{n_S}$ at time moment t_k depends implicitly on the set of parameters $\theta \in \Re^{n_P}$, possibly uncertain (the model has n_S states and n_P parameters). M is the model solution operator which integrates the model equations forward in time (starting from state y_{k-1} at time t_{k-1} to state y_k at time t_k).

For parameter estimation it is convenient to formally extend the model state to include the model parameters and extend the model with trivial equations for parameters (such that parameters do not change during the model evolution)

$$\theta_k = \theta_{k-1} \tag{15}$$

The optimal estimation of the uncertain parameters is thus reduced to the problem of optimal state estimation. We assume that observations of quantities that depend on system state are available at discrete times t_k

$$z_k = h\left(y_k\right) + \varepsilon_k^{obs} \approx H_k y_k + \varepsilon_k^{obs},\quad \left\langle \varepsilon_k^{obs} \right\rangle = 0,\quad \left\langle \left(\varepsilon_k^{obs}\right)\left(\varepsilon_k^{obs}\right)^T \right\rangle = R_k \tag{16}$$

where $z_k \in \Re^{n_O}$ is the observation vector at t_k, h is the (model equivalent) observation operator and H_k is the linearization of h about the solution y_k. Note that there are n_O observations for the n_S-dimensional state vector, and that typically $n_O < n_S$. Each observation is corrupted by observational (measurement and representativeness) errors (Cohn, 1997). We denote by $\langle \cdot \rangle$ the ensemble average over the uncertainty space. The observational error is the experimental uncertainty associated with the measurements and is usually considered to have a Gaussian distribution with zero mean and a known covariance matrix R_k.

The Kalman filter (Evensen, 1992, 1993; Fisher, 2002, Kalman, 1960) assumes that the model (14) is linear, and the model state at previous time t_{k-1} is normally distributed with mean y_{k-1}^a and covariance matrix P_{k-1}^a. The Extended Kalman Filter (EKF) allows for nonlinear models and observations by assuming the error propagation is linear. In the EKF approach, the nonlinear observation operators are linearized, $y_k^{obs} = H_k y_k + \varepsilon_k^{obs}$.

The state is propagated from t_{k-1} to t_k using model equations, and the covariance matrix is explicitly propagated using the tangent linear operator and its adjoint,

$$y_k^f = M\left(t_{k-1}, y_{k-1}^a, p\right),\qquad P_k^f = M' P_{k-1}^a M'^* + Q \tag{17}$$

where the subscripts *f* and *a* stand for forecast and analysis, respectively. M is the model (14) propagator (from t_{k-1} to t_k), M' is the corresponding tangent linear propagator and M'^* is its adjoint. Q represents the covariance of the model errors.

Under linear, Gaussian assumptions, the PDFs of the forecast and assimilated fields are also Gaussian, and completely described by the mean state and the covariance matrix. The assimilated field y_k^a and its covariance matrix P_k^a are computed from the model forecast y_k^f, the current observations y_k^{obs}, and from their covariances using:

$$\begin{aligned} y_k^a &= y_k^f + P_k^f H_k^T \left(R_k + H_k P_k^f H_k^T\right)^{-1} \left(y_k^{obs} - H_k y_k^f\right), \\ P_k^a &= P_k^f - P_k^f H_k^T \left(R_k + H_k P_k^f H_k^T\right)^{-1} H_k P_k^f . \end{aligned} \tag{18}$$

One step of the data assimilation with the extended Kalman filter can be represented as:

$$y_{k-1}^a \text{ and } P_{k-1}^a \xrightarrow{\text{Model \& Tangent Linear Model}} \begin{matrix} y_k^f \text{ and } P_k^f \\ y_k^{obs} \text{ and } R_k \end{matrix} \xrightarrow{\text{Filter}} y_k^a \text{ and } P_k^a \tag{19}$$

For parameter estimation extend the model state to formally include the model parameters:

$$\begin{bmatrix} y_k^f \\ \theta_k^f \end{bmatrix} = \begin{bmatrix} M\left(t_{k-1}, y_{k-1}^a, \theta_{k-1}^a\right) \\ \theta_{k-1}^a \end{bmatrix} \tag{20}$$

The covariance matrix of the extended state vector can be estimated from the polynomial chaos expansions of $y(\xi)$ and $\theta(\xi)$.

$$P_k^f = \operatorname{cov}\left(\begin{bmatrix} y_k^f(\xi) \\ \theta_k^f(\xi) \end{bmatrix}\right) = \begin{bmatrix} \operatorname{cov}\left(y_k^f\right) & \operatorname{cov}\left(y_k^f, \theta_k^f\right) \\ \operatorname{cov}\left(\theta_k^f, y_k^f\right) & \operatorname{cov}\left(\theta_k^f\right) \end{bmatrix} \tag{21}$$

Using this covariance matrix compute the Kalman gain matrix using the formula:

$$K_k = P_k^f H_k^T \left(R_k + H_k P_k^f H_k^T\right)^{-1} \tag{22}$$

The Kalman filter formula computes the assimilated state and parameter vector as:

$$\begin{bmatrix} y_k^a \\ \theta_k^a \end{bmatrix} = \begin{bmatrix} y_k^f \\ \theta_k^f \end{bmatrix} + K_k \left(y_k^{obs} - H_k \begin{bmatrix} y_k^f \\ \theta_k^f \end{bmatrix}\right) = \left(I - K_k H_k\right) \begin{bmatrix} y_k^f \\ \theta_k^f \end{bmatrix} + K_k y_k^{obs} \tag{23}$$

Assuming that no direct observations are made on the parameters, and only the state is observed, we obtain:

$$\begin{bmatrix} y_k^a \\ \theta_k^a \end{bmatrix} = \begin{bmatrix} y_k^f \\ \theta_k^f \end{bmatrix} + K_k \left(y_k^{obs} - H_k y_k^f\right) = \left(I - K_k H_k\right) y_k^f + K_k y_k^{obs} \tag{24}$$

Using the polynomial chaos expansions of the forecast state and the parameters:

$$\begin{bmatrix} y_k^f(\xi) \\ \theta_k^f(\xi) \end{bmatrix} = \begin{bmatrix} \sum_{i=1}^{S} \left(y_k^f\right)^i \psi^i(\xi) \\ \sum_{i=1}^{S} \left(\theta_k^f\right)^i \psi^i(\xi) \end{bmatrix} \tag{25}$$

the Kalman filter formula is used to determine the polynomial chaos expansion of the assimilated model and parameters. For this, first insert the polynomial chaos expansions into the filter formula:

$$\begin{bmatrix} \sum_{i=1}^{S} \left(y_k^a\right)^i \psi^i(\xi) \\ \sum_{i=1}^{S} \left(\theta_k^a\right)^i \psi^i(\xi) \end{bmatrix} = \left(I - K_k H_k\right) \begin{bmatrix} \sum_{i=1}^{S} \left(y_k^f\right)^i \psi^i(\xi) \\ \sum_{i=1}^{S} \left(\theta_k^f\right)^i \psi^i(\xi) \end{bmatrix} + K_k y_k^{obs} \psi^1(\xi) \tag{26}$$

Note that the term with the observations does not depend on the random variables and is therefore associated with only the first (constant) basis function. By a Galerkin projection we see that the polynomial chaos coefficients of the assimilated state and parameters are:

$$\begin{bmatrix} \begin{pmatrix} y_k^a \\ \theta_k^a \end{pmatrix}^i \end{bmatrix} = \left(I - K_k H_k\right) \begin{bmatrix} \begin{pmatrix} y_k^f \\ \theta_k^f \end{pmatrix}^i \end{bmatrix} + K_k y_k^{obs}\, \delta_{i-1}\,, \quad i = 1, \cdots, S \tag{27}$$

If all the observations are made only on the state of the system we have that:

$$\begin{bmatrix} \begin{pmatrix} y_k^a \\ \theta_k^a \end{pmatrix}^i \end{bmatrix} = \left(I - K_k H_k\right) \left(y_k^f\right)^i + K_k y_k^{obs}\, \delta_{i-1}\,, \quad i = 1, \cdots, S \tag{28}$$

The covariance of the extended state vector is:

$$P_k = \mathrm{cov}\left(\begin{bmatrix} y_k \\ \theta_k \end{bmatrix}\right) = \begin{bmatrix} \mathrm{cov}(y_k) & \mathrm{cov}([y_k, \theta_k]) \\ \mathrm{cov}([\theta_k, y_k]) & \mathrm{cov}(\theta_k) \end{bmatrix} = \begin{bmatrix} P_{yy}^k & P_{y\theta}^k \\ P_{\theta y}^k & P_{\theta\theta}^k \end{bmatrix}, \quad \begin{bmatrix} H_k & 0 \end{bmatrix} P_k \begin{bmatrix} H_k^T \\ 0 \end{bmatrix} = H_k P_{yy} H_k^T \tag{29}$$

The Kalman gain reads:

$$K_k = P_k \begin{bmatrix} H_k^T \\ 0 \end{bmatrix} \left(R_k + H_k P_{yy}^k H_k^T\right)^{-1} = \begin{bmatrix} P_{yy}^k H_k^T \\ P_{\theta y}^k H_k^T \end{bmatrix} \left(R_k + H_k P_{yy}^k H_k^T\right)^{-1} \tag{30}$$

The parameter estimate is then:

$$\theta_k^a = \theta_k + P_{\theta y}^k H_k^T \left(R_k + H_k P_{yy}^k H_k^T\right)^{-1} \left(y_k^{obs} - H_k\, y_k\right) \tag{31}$$

In the polynomial chaos framework the covariance matrices P_{yy} and $P_{\theta y}$ can be estimated from the polynomial chaos expansion of the solution and the parameters. Then the polynomial chaos coefficients of the parameters are adjusted as:

$$\left(\theta_k^a\right)^i = \left(\theta_k\right)^i + P_{\theta y}^k H_k^T \left(R_k + H_k P_{yy}^k H_k^T\right)^{-1} \left(y_k^{obs} \cdot \delta_{i-1} - H_k\, y_k{}^i\right), \; i = 1, \cdots, S \tag{32}$$

Let's note that the Kalman filter formula is optimal for the linear Gaussian case. For non-Gaussian uncertainties the Kalman filter formula is sub-optimal, but is still expected to work.

Another possible approach is to apply the filter formula only once, on a vector containing all the observations from t_1 to t_k:

$$\left(\theta^a\right)^i = \left(\theta_0\right)^i + P_{\theta y} H^T \left(R + H P_{yy} H^T\right)^{-1} \left(y_{obs} \cdot \delta_{i-1} - H y^i\right), \; i = 1, \cdots, S \tag{33}$$

where

$$y_{obs} = \left[(y_1^{obs})^T \quad \cdots \quad (y_k^{obs})^T \quad \cdots \quad (y_N^{obs})^T \right]^T \tag{34}$$

$$H = \begin{bmatrix} H_1 & & & (0) \\ & \ddots & & \\ & & H_k & \\ & & & \ddots \\ (0) & & & H_N \end{bmatrix} \tag{35}$$

$$R = \begin{bmatrix} R_1 & & (0) \\ & \ddots & \\ & R_k & \\ & & \ddots \\ (0) & & R_N \end{bmatrix} \tag{36}$$

$$P_{\theta y} = \mathrm{cov}\left([\theta_0, y]\right),\ P_{yy} = \mathrm{cov}(y),\ \text{ with } \ y = \left[(y_1)^T \quad \dots \quad (y_k)^T \quad \dots \quad (y_N)^T\right]^T \tag{37}$$

The original approach will be called the one-time-step-at-a-time EKF approach, and this alternative approach will be called the whole-set-of-data-at-once EKF approach. The two approaches are equivalent only for linear systems with Gaussian assumptions. Even in that case, they might not always be equivalent in practice, due to numerical issues.

3. Insight into the EKF approach using simple mechanical systems

3.1 Roll plane modeling of a vehicle

The model used to apply the theory presented in this article is based on the four degree of freedom roll plane model of a vehicle used by Simon (1999) with the addition of a mass on the roll bar, as shown in Figure 1. The difference is that the suspension dampers and the suspension springs used in this study are nonlinear and that a mass is added on the roll bar, which represents the driver, the passenger, and other objects in the vehicle. The added mass M and its position d_{CG} away from the left end of the roll bar are assumed to be uncertain. It is assumed that there is a passenger, and apriori distribution of the added mass will therefore be centered in the middle of the bar. This added mass will be represented as a point mass for the sake of simplicity. Measuring the position of the C.G. of the added mass physically is not straightforward. However, if a well defined road input can be used and sensors are available, these two parameters can be estimated based on the observed displacements and velocities across the suspensions.

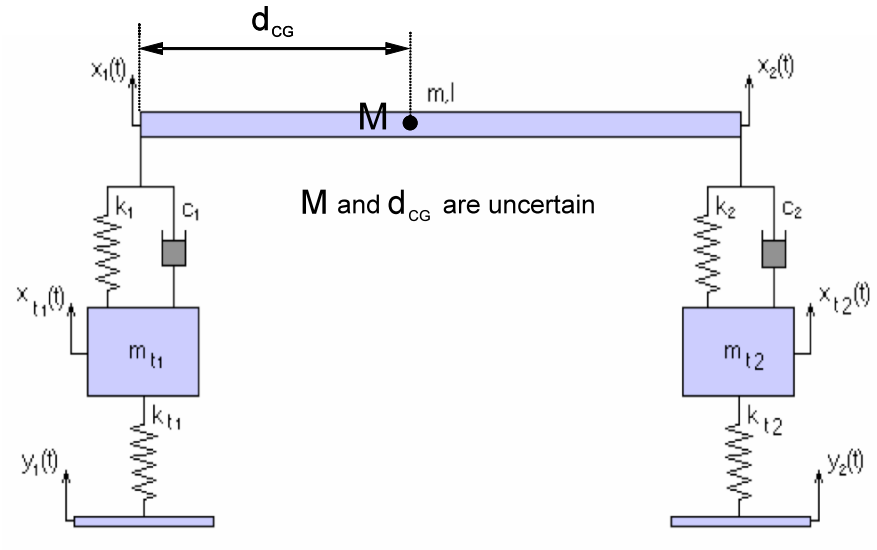

Figure 1. Four degree of freedom roll plane model (adapted from the model used by Simon (1999))

The body of the vehicle is represented as a bar of mass m (sprung mass) and length l that has a moment of inertia I. The unsprung masses, i.e., the masses of each tire/axle combination, are represented by m_{t1} and m_{t2}. A mass

is added on the roll bar, which represents the driver and other objects in the vehicle. That added mass is represented as a point mass of value M situated at a distance d_{CG} from the left extremity of the roll bar.

The motion variables x_1 and x_2 correspond to the vertical position of each side of the vehicle body, while the motion variables x_{t1} and x_{t2} correspond to the position of the tires.

The inputs to this system are y_1 and y_2, which represent the road profile under each wheel.

If x is the relative displacement across the suspension spring with a stiffness k_i (i = 1, 2), the force across the suspension spring is given by:

$$F_{K_i}(x) = k_i x + k_{i,3} x^3, \quad i = 1, 2 \tag{38}$$

If v is the relative velocity across the damper with a damping coefficient c_i (i = 1, 2), the force across the damper is given by:

$$F_{C_i}(v) = c_i (0.2 \tanh(10v)) \tag{39}$$

For small angles, i.e. for $\frac{x_2 - x_1}{L}$ small, the equations of motion of the system are

$$\left(\frac{m+M}{2}\right)\left(\ddot{x}_2 + \ddot{x}_1 + (\ddot{x}_2 - \ddot{x}_1)\frac{M}{(m+M)}\left(2(d_{CG}/L) - 1\right)\right) + F_{K_1}(x_1 - x_{t1}) + F_{K_2}(x_2 - x_{t2}) + F_{C_1}(\dot{x}_1 - \dot{x}_{t1}) + F_{C_2}(\dot{x}_2 - \dot{x}_{t2}) = 0 \tag{40}$$

$$\cos\left(\left(\frac{x_2 - x_1}{L}\right) + \left(\frac{x_2 - x_1}{L}\right)_{STATIC}\right) \times \left[D\left(F_{K_1}(x_1 - x_{t1}) + F_{C_1}(\dot{x}_1 - \dot{x}_{t1})\right) - (L - D)\left(F_{K_2}(x_2 - x_{t2}) + F_{C_2}(\dot{x}_2 - \dot{x}_{t2})\right) + g\left(M(D - d_{CG}) - m\left(\frac{L}{2} - D\right)\right) \right] + \left(I + m\left(\frac{L}{2} - D\right)^2 + M(D - d_{CG})^2\right)\left(\frac{\ddot{x}_2 + \ddot{x}_1}{L}\right) = 0 \quad with \quad D = \frac{M\, d_{CG} + m\,(L/2)}{M + m} \tag{41}$$

$$m_{t1}\ddot{x}_{t1} + F_{K_1}(x_{t1} - x_1) + F_{C_1}(\dot{x}_{t1} - \dot{x}_1) = k_{t1}(y_1 - x_{t1}) \tag{42}$$

$$m_{t2}\ddot{x}_{t2} + F_{K2}(x_{t2} - x_2) + F_{C_2}(\dot{x}_{t2} - \dot{x}_2) = k_{t2}(y_2 - x_{t2}) \tag{43}$$

where F_{K_1}, F_{K_2}, F_{C_1}, and F_{C_2} are defined in equations (38) and (39).

In these equations, the variables are expressed versus their position at equilibrium (if the added mass M is not in the middle, we have static deflections). $\left(\frac{x_2 - x_1}{L}\right)_{STATIC}$ is relative to the position of the ground, which is fixed. It has to be estimated numerically because of the nonlinearities in the system.

The parameters used in this study are shown in Table I. They are the parameters used by Simon (1999), with the addition of nonlinearities and uncertainties for M and d_{CG}. For the parameters shown in Table I, the minimum static angle (i.e., the angle of the roll bar with respect to a fixed reference on the ground) is - 1.21 degrees and the maximum static angle is 1.21 degrees, which corresponds to $x_2 - x_1 = 0.032$ m. These values are obtained for $(\xi_1, \xi_2) = (1, 1)$ and $(\xi_1, \xi_2) = (1, -1)$, i.e.. for the maximum possible value of M with the added mass as far as possible from the center of the bar.

Table I. Vehicle parameters

Parameter	Description	Value
m	Mass of the Roll Bar	580 kg
m_{t1}, m_{t2}	Mass of the tire/axle	36.26 kg
c_1, c_2	Damping coefficients	710.70 N s /m
k_1, k_2	Spring constants – linear component	19,357.2 N/m
$k_{1,3}$, $k_{2,3}$	Spring constants – cubic component	100,000 N/m^3
l	Length of the Roll Bar	1.524 m
I	Inertia of the Roll Bar	63.3316 kg m^2
k_{t1}, k_{t2}	Tires vertical stiffnesses	96,319.76 N/m
M	Added Mass	200 kg +/-50%, with Beta (2, 2) distribution
d_{CG}	Distance between the C.G. of the mass and the left extremity of the roll bar	0.7620 m +/-25%, with Beta (2, 2) distribution

The uncertainties of 50% and 25% on the values of M and d_{CG} can be represented as:

$$M = M_{nom}(1 + 0.50\,\xi_1), \quad \xi_1 \in [-1,\ 1] \tag{44}$$

$$d_{CG} = d_{CG,nom}(1 + 0.25\,\xi_2), \quad \xi_2 \in [-1,\ 1] \tag{45}$$

where M_{nom} and $d_{CG,nom}$ are the nominal values of the vertical stiffnesses of the tires ($M_{nom} = 200\,\text{kg}$ and $d_{CG,nom} = 0.7620\,\text{m}$).

It is assumed that the probability density functions of the values of M and d_{CG} can be represented with Beta (2, 2) distributions (Sandu *et al.*, 2006 a, 2006 b), with uncertainties of +/- 50% and +/- 25%, respectively. The distributions of the uncertainties related to the values of M and d_{CG}, defined on the interval $[-1,\ 1]$, are represented in Figure 2. They have the following Probability Density Functions (PDFs):

$$w(\xi_i) = \frac{3}{4}\left(1 - \xi_i^{\,2}\right), \quad i = 1, 2 \tag{46}$$

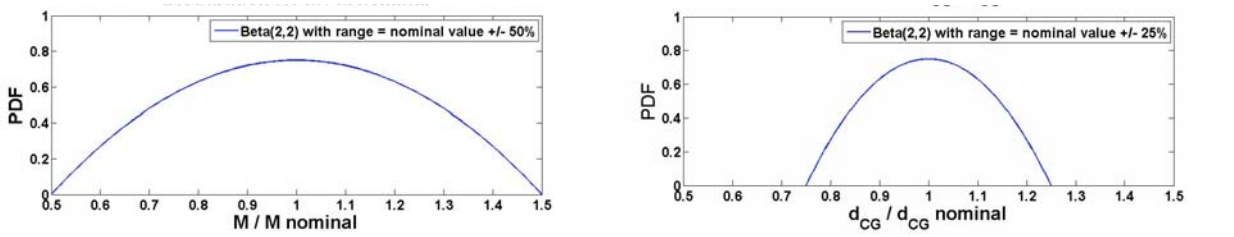

(a) **(b)**

Figure 2. Beta (2, 2) distribution

Notes: a) for value of the mass, b) for value of the position of the C.G. of the mass

3.2 Collocation points

The generalized polynomial chaos theory is explained by Sandu *et al.* (2006 a) in which direct stochastic collocation is proposed as a less expensive alternative to the traditional Galerkin approach. The collocation approach consists of imposing that the equations system holds at a given set of collocation points. If the polynomial chaos expansions contain 15 terms for instance, then at least 15 collocation points are needed in order to have at least 15 equations for 15 unknown polynomial chaos coefficients. It is desirable to have more collocation points than polynomial coefficients to solve for. In that case a least-squares algorithm is used to solve the system with more equations than unknowns.

Unless otherwise specified, in this study, the polynomial chaos expansions of M and d_{CG} will use 15 terms. All the other variables affected by the uncertainties on M and d_{CG} will be modeled by a polynomial chaos expansion using 15 terms as well. The collocation approach is the one used in this study. It requires at least 15 collocation points to derive the coefficients associated to each of the 15 terms of the different polynomial chaos expansions.

Unless otherwise specified, 30 collocation points will be used in this study to derive the coefficients associated to each of the 15 terms of the different polynomial chaos expansions. The collocation points used in this study are obtained using an algorithm based on the Halton algorithm (Halton and Smith, 1964), which is similar to the Hammersley algorithm (Hammersley, 1960). These collocation points for a uniform distribution are shown in Figure 3(a).

One of the advantages of the Hammersley/Halton points used in this study is that when the number of points is increased, the new set of points still contains all the old points. We therefore know that more points should result in a better approximation. The collocation points for a Beta (2, 2) distribution, which is used in this study, are shown in Figure 3(b).

The transformation from the collocation points for a uniform distribution to the points for a Beta (2, 2) distribution is achieved by applying the inverse Cumulative Distribution Function of the Beta (2, 2) distribution. Let's note that there is no collocation point at the boundary, i.e., no point associated with an uncertainty equal to -1 or 1, which is needed in order to avoid having a cost function equal to infinity.

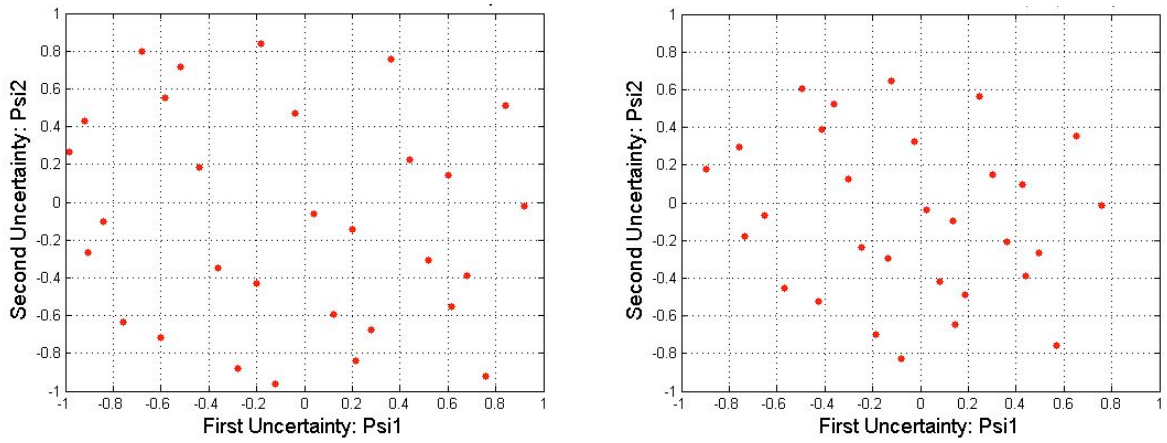

(a) **(b)**

Figure 3. Halton collocation points (2 dimensions, 30 points)

Notes: a) for uniform distribution, b) for beta (2, 2) distribution

3.3 Experimental setting – road input

In order to assess the efficiency of the polynomial chaos theory for parameter estimation, M and d_{CG} will be estimated using observations of four motion variables obtained for a given road input: the displacements across the suspensions ($x_1 - x_{t1}$ and $x_2 - x_{t2}$), and their corresponding velocities ($\dot{x}_1 - \dot{x}_{t1}$ and $\dot{x}_2 - \dot{x}_{t2}$). The road profile is shown in Figure 4, and the road input is obtained assuming the vehicle has a constant speed of 16 km/h (10 mph). The road profile can be

seen as a long speed bump. The first tire is subjected to a ramp at $t = 0$, and reaches a height of 10 cm (4") for a horizontal displacement of 1m, then stays at the same height for 1m, and goes back down to its initial height. The second tire is subjected to the same kind of input, but with a time delay of 20% and it reaches a maximum height of only 8 cm.

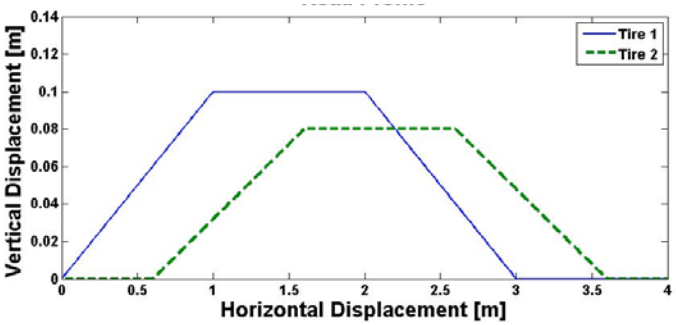

Figure 4. Road profile – speed bump

The four motion variables are plotted from $t = 0$ to $t = 3$ seconds using $M^{ref} = 223.26\,\text{kg}$ and $d_{CG}{}^{ref} = 0.6882\,\text{m}$ (i.e., $\xi_1{}^{ref} = 0.2326$ and $\xi_2{}^{ref} = -0.3875$) and assuming these values can only be measured with a sampling rate of $0.3\,\text{s}$.

However, for the proof of concept of the parameter estimation method presented in this paper, we pretend we do not know the values of M and d_{CG}, the objective being to estimate those values based on the plot of the four motion variables shown in Figure 5. Let's note that three seconds of data correspond to a horizontal displacement of 13.33 meters. The end of the speed bump occurs at $t = 0.675\,\text{s}$.

The excitation signal is supposed to be perfectly known. In other words, the road profile shown in Figure 4 is supposed to be exactly known and the speed of the vehicle is supposed to be exactly 16 km/h at all time, which enables us to use any desired sampling rate for the input signal. However, only 10 measurement points are used for the output displacements and velocities (not counting the measurements at $t = 0$, which give no useful information in order to estimate the unknown parameter).

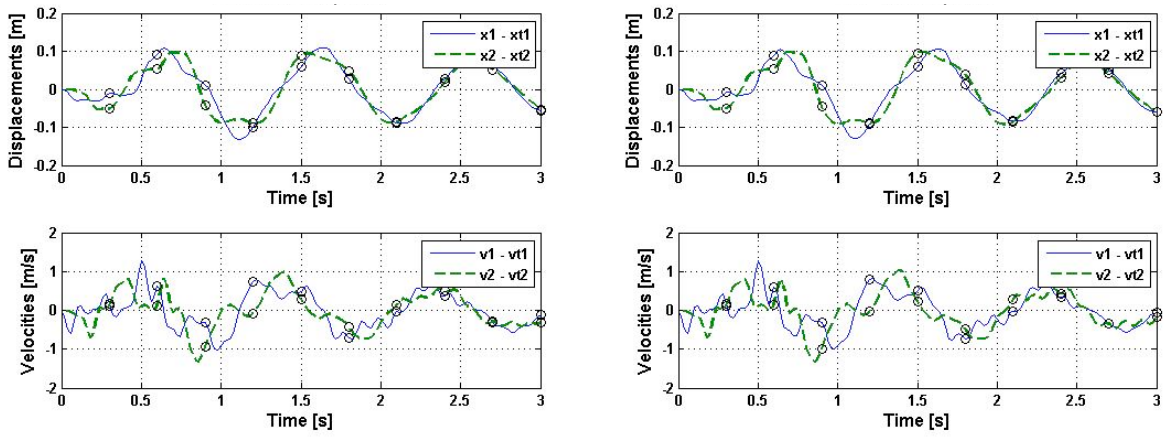

(a) **(b)**

Figure 5. Observed states - displacements and velocities:

Notes: a) measured, b) for nominal values ($\xi_1 = 0$, $\xi_2 = 0$)

Inaccurate estimates can be caused by different factors, including a sampling rate below the Nyquist frequency, non-identifiability, non-observability, and an excitation signal that is not rich enough (Blanchard *et al.*, 2007c). The four degree of freedom roll plane model used in this article is exactly the same than the one used by Blanchard *et al.* (2007d). The road inputs used in this article have also been used by Blanchard *et al.* (2007d), who showed it is possible to perform parameter estimation even when using only 10 time points for 3 seconds of data (i.e., a sampling rate of 0.3s).

The measurements shown in Figure 5(a) are synthetic measurements obtained from a reference simulation with the reference value of the uncertain parameter $\xi_1^{ref} = 0.2326$ and $\xi_2^{ref} = -0.3875$. Parameters estimation is performed using the EKF approach. In order to work with a realistic set of measurements, a Gaussian measurement noise with zero mean and 1% variance is added to the observations shown in Figure 5 (for the relative displacements and velocities) before performing parameter estimation.

The state of the system at future times depends on the random initial velocity and can be represented by

$$y(\xi,t) = \left[x_1(\xi,t) \quad x_2(\xi,t) \quad x_{t1}(\xi,t) \quad x_{t2}(\xi,t) \quad \frac{dx_1(\xi,t)}{dt} \quad \frac{dx_2(\xi,t)}{dt} \quad \frac{dx_{t1}(\xi,t)}{dt} \quad \frac{dx_{t2}(\xi,t)}{dt} \quad \theta(\xi,t) \right]^T \tag{47}$$

If we assume that only the displacements across the suspensions ($x_1 - x_{t1}$ and $x_2 - x_{t2}$), and their corresponding velocities ($\dot{x}_1 - \dot{x}_{t1}$ and $\dot{x}_2 - \dot{x}_{t2}$) can be measured, then

$$H = \begin{bmatrix} 1 & 0 & -1 & 0 & 0 & 0 & 0 & 0 & 0 \\ 0 & 0 & 0 & 0 & 1 & 0 & -1 & 0 & 0 \\ 0 & 1 & 0 & -1 & 0 & 0 & 0 & 0 & 0 \\ 0 & 0 & 0 & 0 & 0 & 1 & 0 & -1 & 0 \end{bmatrix} \tag{48}$$

and the measurements yield

$$z_k = H \cdot y^{\text{ref}}(t_k) + \varepsilon_k = x^{\text{ref}}(t_k) + \varepsilon_k, \quad \varepsilon_k \in \mathrm{N}(0, R_k). \tag{49}$$

Measurement errors at different times are independent random variables. The measurement noise ε_k is assumed to be Gaussian with a zero mean and a variance 1% of the value of $x(t)$. The diagonal elements of the covariance matrix of the uncertainty associated with the measurements will still be set to at least 10^{-12} when necessary so that R_k^{-1} can always be computed. Therefore, the covariance of the uncertainty associated with the measurements is

$$R_k = \begin{bmatrix} R_{k1} & 0 & 0 & 0 \\ 0 & R_{k2} & 0 & 0 \\ 0 & 0 & R_{k3} & 0 \\ 0 & 0 & 0 & R_{k4} \end{bmatrix} \tag{50}$$

where

$$R_{k1} = \max\left\{10^{-12}, (0.01\ z_{k1})^2\right\} \tag{51}$$

$$R_{k2} = \max\left\{10^{-12}, (0.01\ z_{k2})^2\right\} \tag{52}$$

$$R_{k3} = \max\left\{10^{-12}, (0.01\ z_{k3})^2\right\} \tag{53}$$

$$R_{k4} = \max\left\{10^{-12}, (0.01\ z_{k4})^2\right\} \tag{54}$$

The estimated values of ξ_1 and ξ_2 obtained using the one-time-step-at-a-time EKF approach, which are given by the first terms of the corresponding polynomial chaos expansions, are $\xi_1^{est} = 0.2240$ and $\xi_2^{est} = -0.4415$, i.e., $M^{est} = 222.40\,\text{kg}$ and $d_{CG}{}^{est} = 0.6779\,\text{m}$, which seems to be a good estimation considering that only 10

measurement points were used and that there is noise associated to the measurements. The actual values were $\xi_1^{ref} = 0.2326$ and $\xi_2^{ref} = -0.3875$, i.e., $M^{ref} = 223.26$ kg and $d_{CG}^{ref} = 0.6882$ m. The EKF estimations come in the form of PDFs, as shown in Figure 6(a) for M, and Figure 6(b) for d_{CG}. The estimated values and the corresponding standard deviations at each time step are plotted in Figure 6(c) for M, and Figure 6(d) for d_{CG}. Let's remember that the standard deviations are given by equation (11).

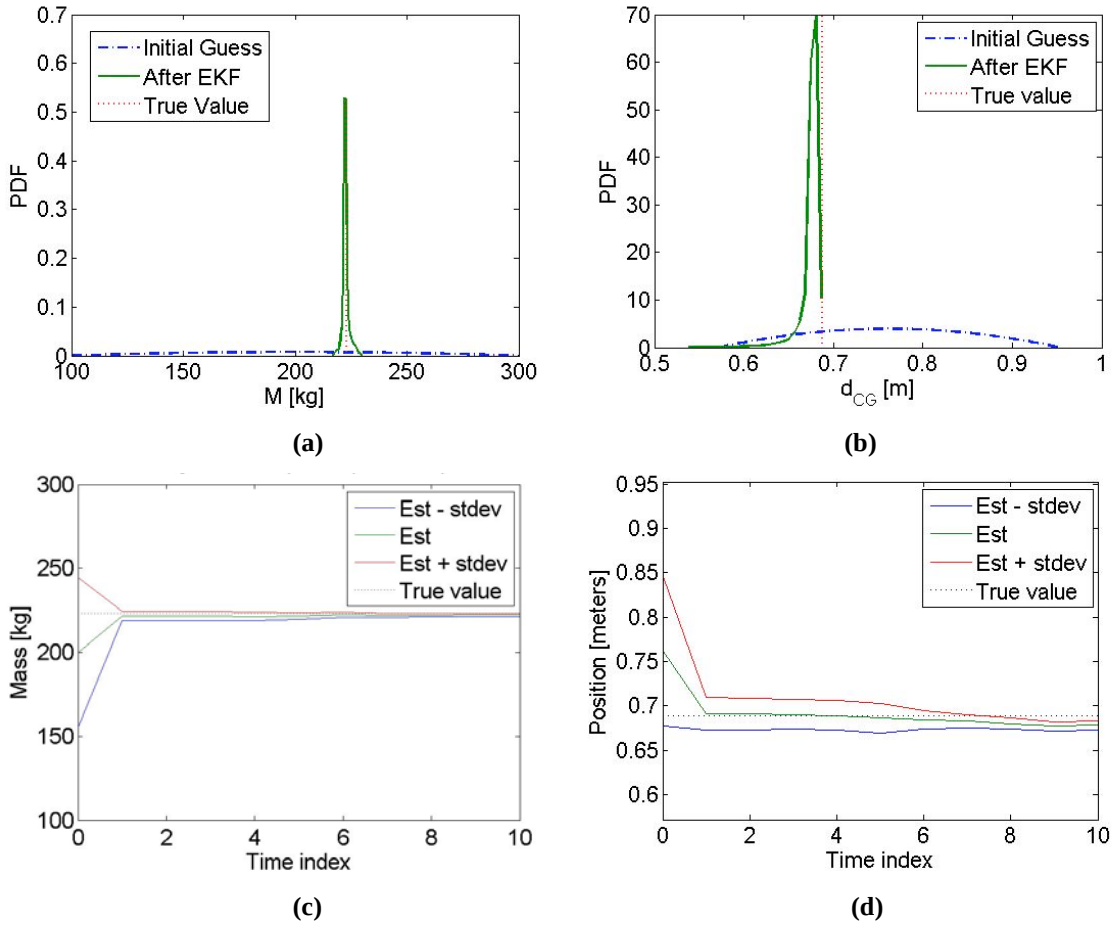

Figure 6. EKF estimation (one time step at a time) for speed bump input with 10 time points (noise = 1%):

Notes: a) Mass in the form of PDF, b) Distance in the form of PDF; c) Mass for each term index, d) Distance for each term index

With 100 sample points (i.e., with time steps of 0.03 s instead of 0.3 s) and a noise level of 1%, the estimated values of ξ_1 and ξ_2 obtained using the one-time-step-at-a-time EKF approach are $\xi_1^{est} = 0.3988$ and $\xi_2^{est} = -0.0834$, i.e., $M^{est} = 239.88$ kg and $d_{CG}^{est} = 0.7461$ m. This is illustrated in Figure 7, which shows that the one-time-step-at-a-time EKF approach does not work anymore when using a time step of 0.03 s instead of 0.3 s. Figure 8 shows the absolute error for our two estimated parameters, i.e., $\left|\xi_{1,est} - \xi_{1,ref}\right|$ and $\left|\xi_{2,est} - \xi_{2,ref}\right|$, with respect to the number of time points, and equivalently, the length of the time step, which is inversely proportional to the number of time points. It can be observed that a long time step is not really desirable, which one would expect since less information is available for longer time steps. However, a short time step is even less desirable. This seems to be counterintuitive since one would expect that more information would yield more accurate results. The problem is that the EKF can diverge when using a high sampling frequency. When applying the polynomial chaos theory to the Extended Kalman Filter (EKF),

numerical errors can accumulate even faster than in the general case due to the truncation in the polynomial chaos expansions. It is shown in Appendix that for the simple scalar system $y' = a\,y$ with $a < 0$ (where a is known), the truncations in the polynomial chaos expansions can prevent the convergence of the covariance of the assimilated state y_a. It is also shown in Appendix that the covariance of the error after assimilation $E_k^a = y_k^a - y_{tk}^{true}$ decreases with the time step Δt when there is no model error (which is the case for this study), meaning that using means a larger Δt results in a smaller error (unless the covariance of y_a has not converged yet, which can happen when Δt is too large). Figures 7(c) and 7(d), which plot the estimated values of the two parameters +/- their standard deviations, show that the results with a time step of 0.03 s could not be trusted, because the EKF was diverging. Indeed, the range of values spanned by the estimated values +/- their standard deviations at time index k does not always include the range of values spanned by the estimated values +/- their standard deviations at time index $k+1$. The curves representing the estimated values +/- the standard deviations of the estimations can decrease and suddenly increase with new observations or vice versa, unlike what was observed in Figures 6(c) and 6(d), where the curves representing the estimated values +/- their standard deviations smoothly decrease/increase. Therefore, it is judicious to look at the estimated values and their standard deviations at each time step. When the estimated values +/- their standard deviations display non-monotonous behaviors, it is a sign that the sampling frequency should be decreased. Sampling below the Nyquist frequency is usually a necessity in order to prevent the EKF from diverging. In most cases, sampling below the Nyquist frequency does not result in non-identifiability issues, but it can in a few rare cases, as illustrated in Blanchard *et al.*, 2007c.

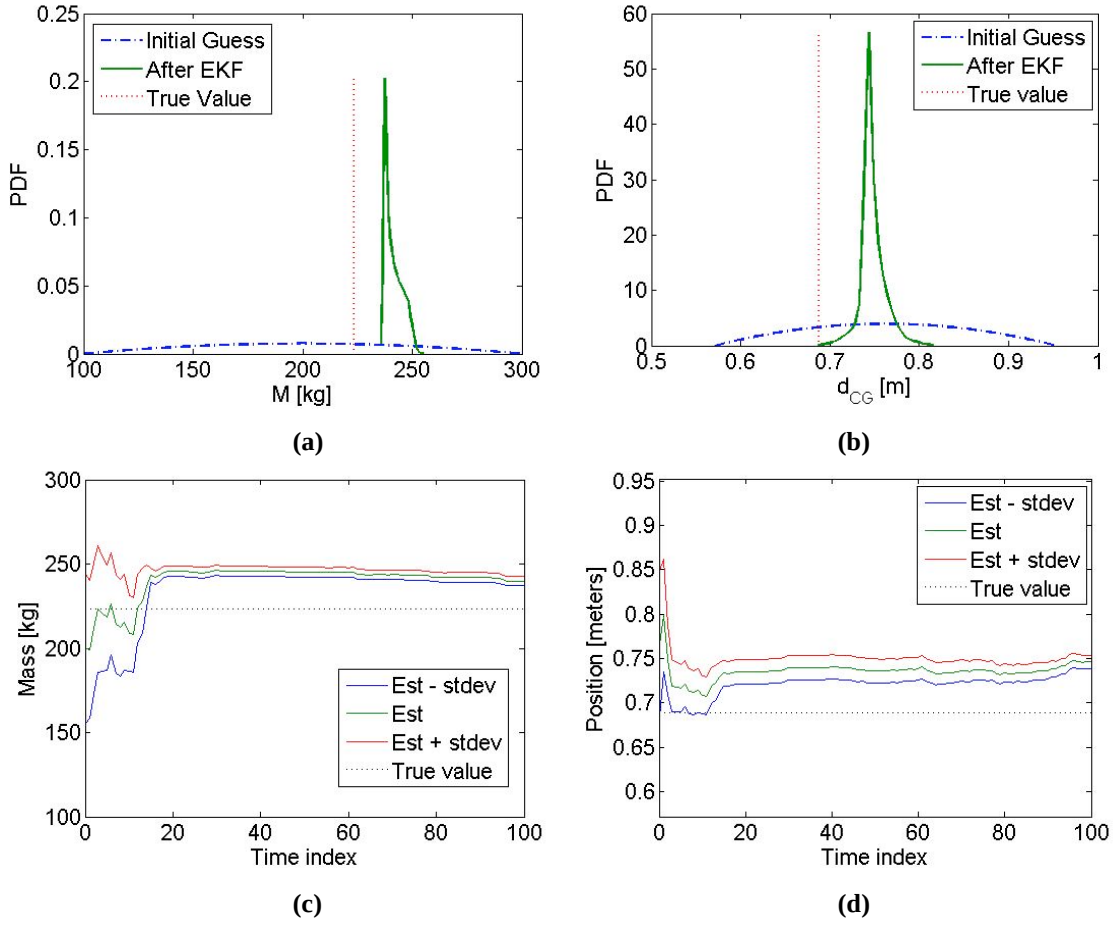

Figure 7. EKF estimation (one time step at a time) for speed bump input with 100 time points (noise = 1%):

Notes: a) Mass in the form of PDF, b) Distance in the form of PDF; c) Mass at each time index, d) Distance at each time index

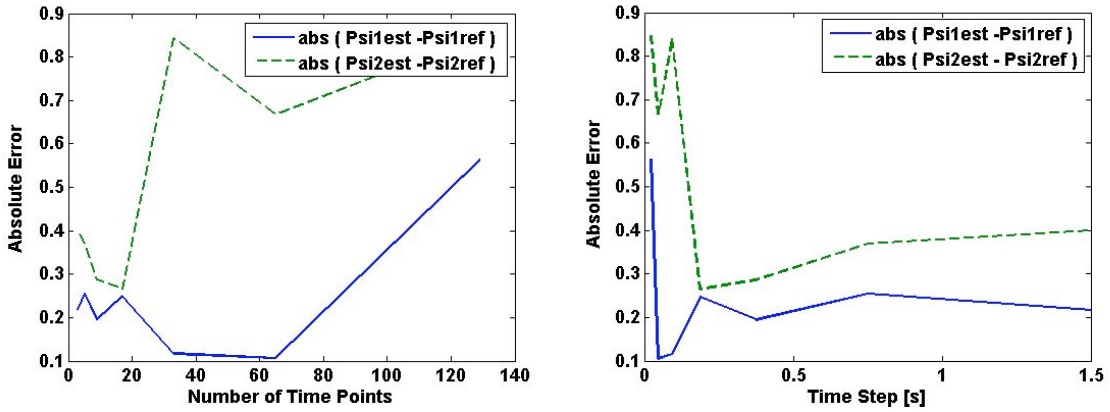

(a) **(b)**

Figure 8. Absolute error for the estimated parameters ξ_1 and ξ_2 with the nonlinear half-car model for the speed bump with respect to: (a) the number of time points; (b) the length of the time step

Another possible approach is to apply the filter formula only once, on a vector containing all the observations from t_1 to t_k. Using this alternative approach, we get better results with a Gaussian measurement noise with zero mean and 1% variance, for both 10 time points (Figure 9) and 100 time points (Figure 10). Applying the EKF formula on the whole set of data at once with 10 time points yields $\xi_1^{\,est} = 0.2321$ and $\xi_2^{\,est} = -0.3969$, i.e., $M^{\,est} = 223.21\,\text{kg}$ and $d_{CG}^{\;\;est} = 0.6864\,\text{m}$. Applying the EKF formula on the whole set of data at once with 100 time points yields $\xi_1^{\,est} = 0.2305$ and $\xi_2^{\,est} = -0.3773$, i.e., $M^{\,est} = 223.05\,\text{kg}$ and $d_{CG}^{\;\;est} = 0.6901\,\text{m}$. For this particular road input, applying the filter formula only once, on a vector containing all the observations clearly yields better results, and this whole-set-of-data-at-once EKF approach still works with a sampling rate of 0.03 s, while the one-time-step-at-a-time EKF approach was clearly not working.

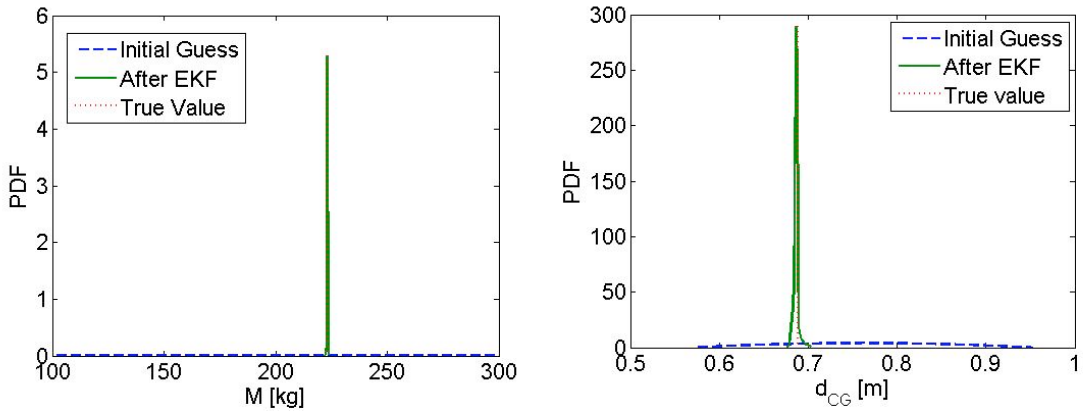

(a) **(b)**

Figure 9. EKF estimation (whole set of data at once) for speed bump input with 10 time points (noise = 1%):

Notes: a) Mass in the form of PDF, b) Distance in the form of PDF

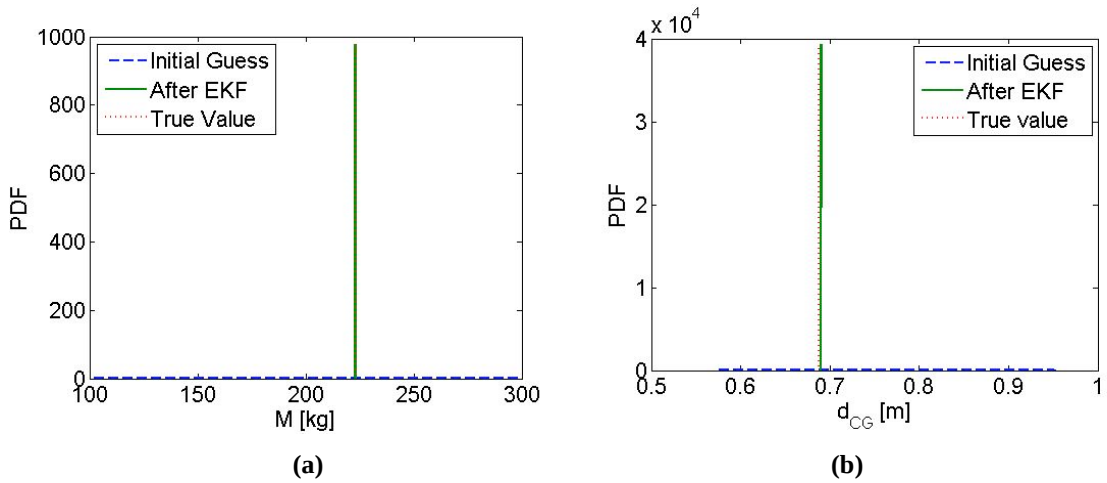

(a) **(b)**

Figure 10. EKF estimation (whole set of data at once) for speed bump input with 100 time points (noise = 1%):

Notes: a) Mass in the form of PDF, b) Distance in the form of PDF

3.4 Experimental setting – out of phase sine input signals at 1 Hz

In order to continue assessing the efficiency of the polynomial chaos theory for parameter estimation, the estimations will now be performed for a 1-Hz harmonic input, with amplitudes of +/- 0.05 m for y_1 and y_2. The input signal is supposed to be exactly known, which enables us to use any desired sampling rate for the input signal. Figure 11 shows the harmonic inputs that will be used at 1 Hz. The parameters M and d_{CG} will still be estimated using a plot of four motion variables: the displacements across the suspensions ($x_1 - x_{t1}$ and $x_2 - x_{t2}$), and their corresponding velocities ($\dot{x}_1 - \dot{x}_{t1}$ and $\dot{x}_2 - \dot{x}_{t2}$). A Gaussian measurement noise with zero mean and 1% variance is still added to the observations.

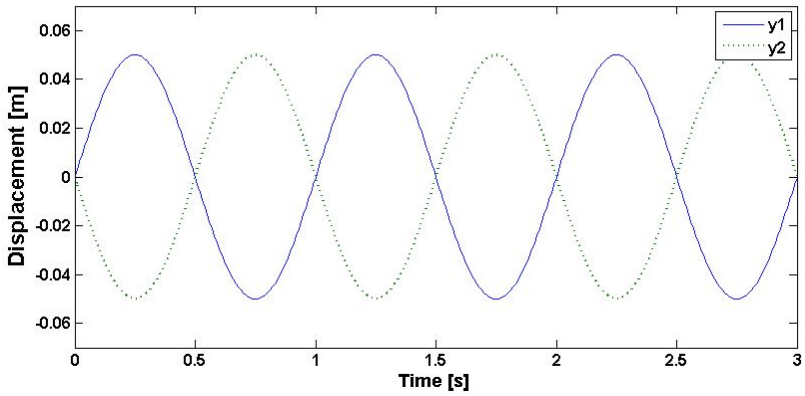

Figure 11. Road input at 1 Hz

Figure 12 shows the results obtained when using the one-time-step-at-a-time EKF approach with 10 time points, i.e., with a sampling rate of 0.3 s. Figure 12(c) shows that the estimation of the mass should actually not be trusted for the reasons explained previously. It can also be observed in Figure 12(a): the PDF contains values above 300 kg, i.e., outside the range of the Beta(2,2) distribution, which means the filter has converge problems. Figure 13 shows the results obtained when using the whole-set-of-data-at-once EKF approach with the same 10 time points. It yields better results for the estimation of the distance, but not for the estimation of the added mass. This shows that this alternative

approach does not necessarily work better for every problem, even though it often yields better results, as it clearly did with the speed bump used in section 3.3.

Figure 14 shows the results obtained when using the one-time-step-at-a-time EKF approach with 100 time points, i.e., with a sampling rate of 0.03 s. The filter clearly diverges and the estimations cannot be trusted, which is especially evident for the estimation of the mass. Figure 15 shows the results obtained when using the whole-set-of-data-at-once EKF approach with the same 100 time points. The estimation of the mass comes with a large standard deviation, but this approach actually yields an acceptable estimation for the mass: $M^{est} = 221.12$ kg ($\xi_1^{est} = 0.2112$). In this case, the whole-set-of-data-at-once EKF approach yields better results with 100 time points than with 10 time points. However, the whole-set-of-data-at-once approach still does not solve all the drawbacks associated with the use of an EKF. It can be observed that the PDF contains values outside the range of the Beta(2,2) distribution, i.e., below 100 kg or above 300 kg, so the convergence problems also appear to affect the whole-set-of-data-at-once approach. When the whole-set-of-data-at-once approach yields a PDF with a large range of possible values, it is not clear how much it can be trusted. As a conclusion, the EKF estimation obtained when applying the filter formula only once on the whole set of data can sometimes yield much better results, but not always, so comparing the results to a different approach (e.g., a Bayesian approach) is strongly recommended.

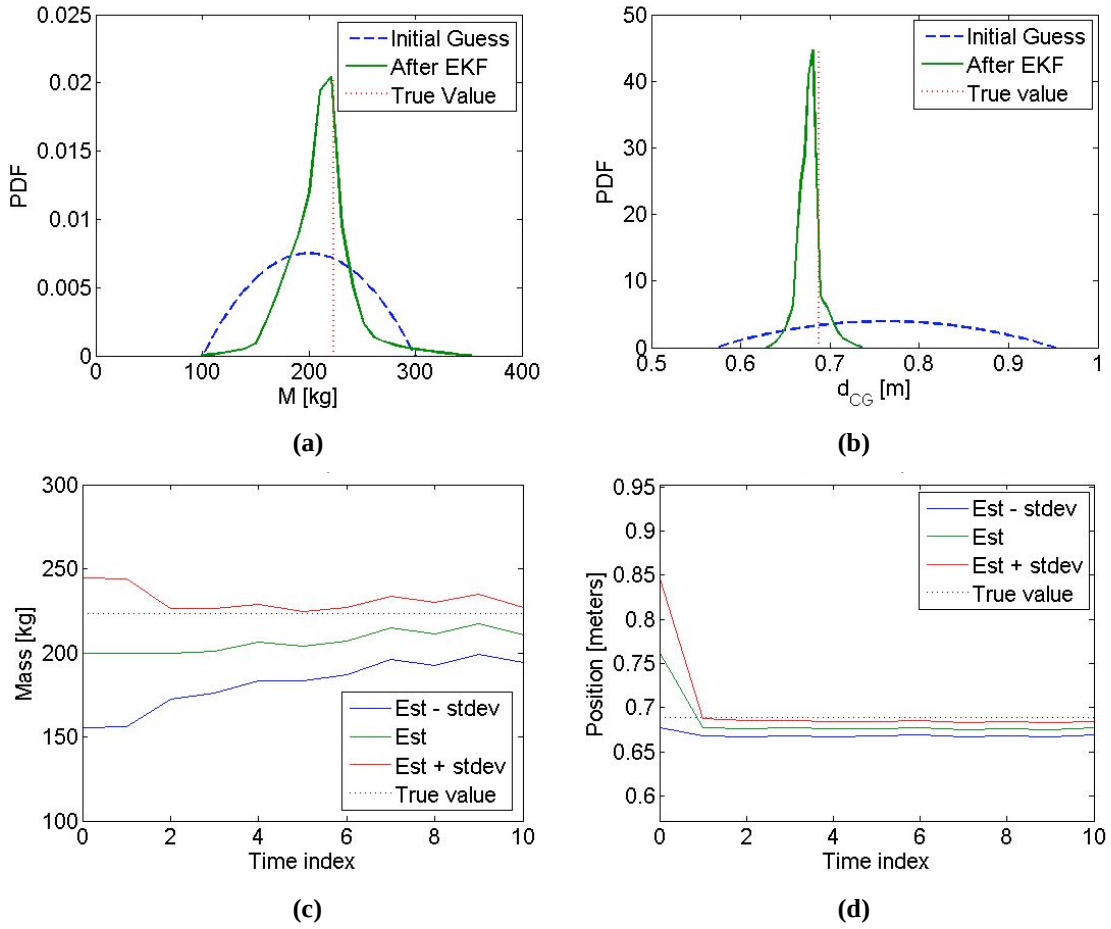

Figure 12. EKF estimation (one time step at a time) at 1 Hz with 10 time points (noise= 1%):

Notes: a) Mass in the form of PDF, b) Distance in the form of PDF; c) Mass at each time index, d) Distance at each time index

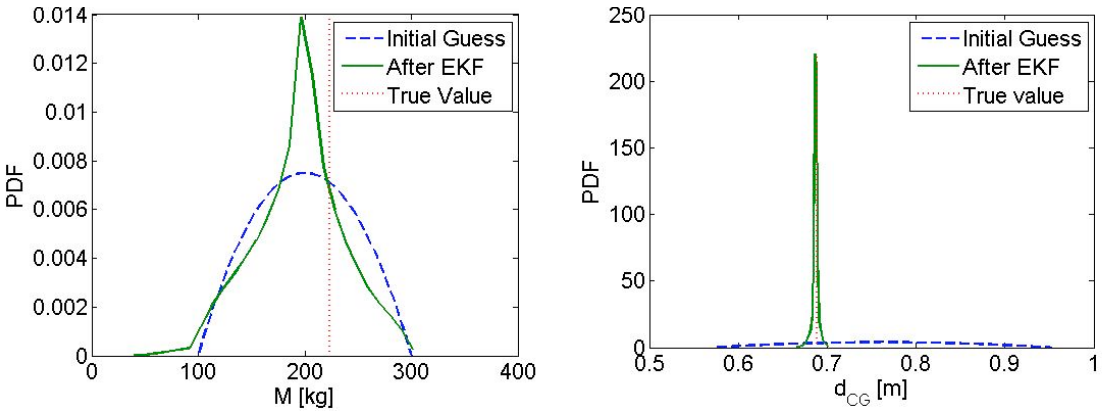

(a) **(b)**

Figure 13. EKF estimation (whole set of data at once) at 1 Hz with 10 time points (noise= 1%):

Notes: a) Mass in the form of PDF, b) Distance in the form of PDF

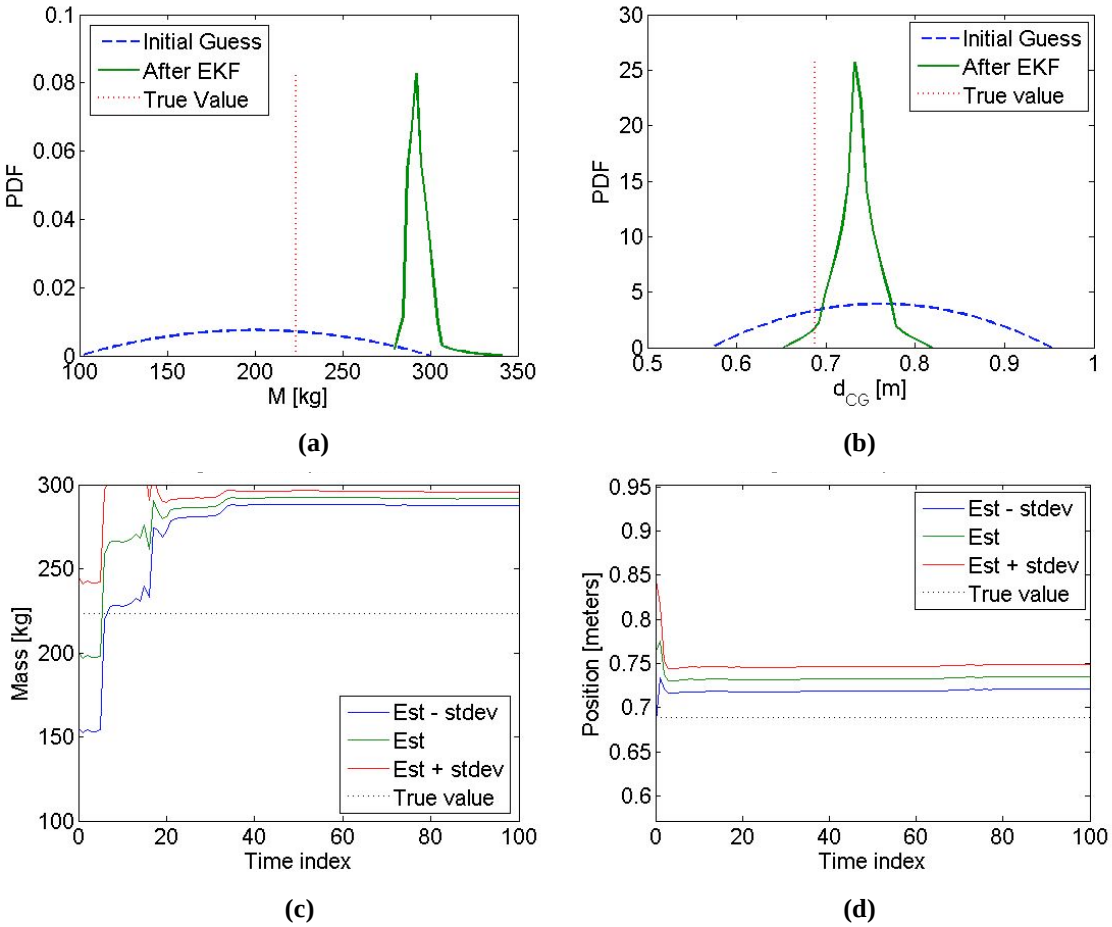

(a) **(b)**

(c) **(d)**

Figure 14. EKF estimation (one time step at a time) at 1 Hz with 100 time points (noise= 1%):

Notes: a) Mass in the form of PDF, b) Distance in the form of PDF; c) Mass at each time index, d) Distance at each time index

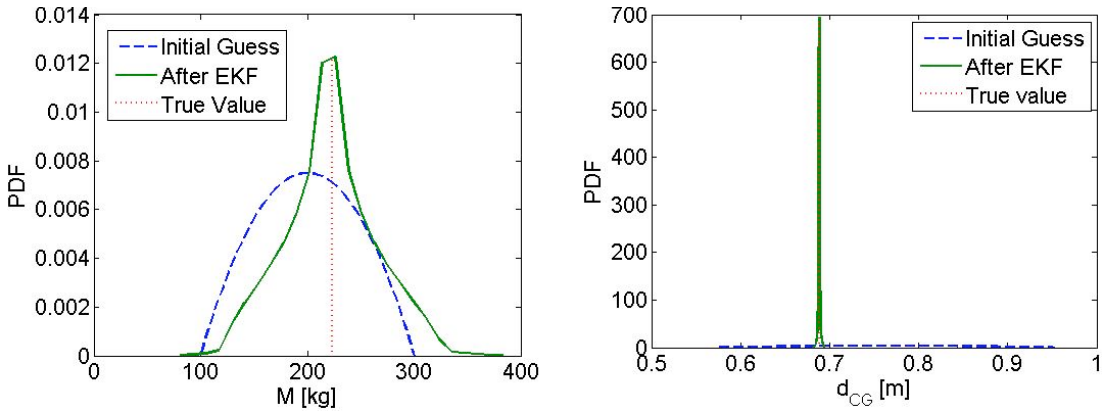

(a) **(b)**

Figure 15. EKF estimation (whole set of data at once) at 1 Hz with 100 time points (noise= 1%):

Notes: a) Mass in the form of PDF, b) Distance in the form of PDF

Parameter estimation can be performed for the same system using linear springs and dampers. Let's use $F_{C_i}(v) = c_i v$ for the dampers and $k_{i,3} = 0$ for the suspension springs (i = 1, 2). It can be observed that the PDFs obtained for the linear case and the nonlinear case are quite similar, as shown as in Figure 16 (which needs to be compared with Figure 13 for the nonlinear case) and Figure 17 (which needs to be compared with Figure 15 for the nonlinear case). For this 1Hz- road input, the problems we encountered do not seem to come from the nonlinearities in the springs and dampers. Nonlinearities can result in a non-identifiable system, but this was not the case for this 1-Hz input, as shown in Blanchard *et al.* (2007d).

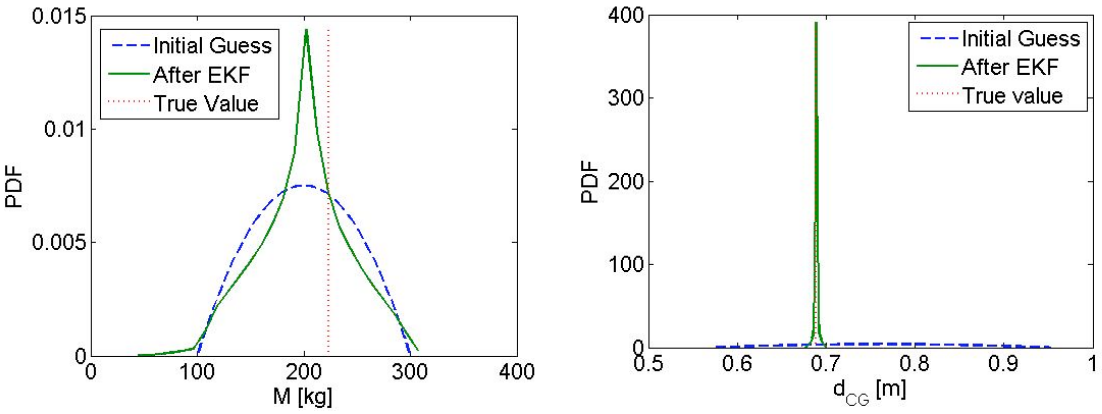

(a) **(b)**

Figure 16. EKF estimation (whole set of data at once) for the linearized system at 1 Hz with 10 time points (noise = 1%): **Notes:** a) Mass in the form of PDF, b) Distance in the form of PDF

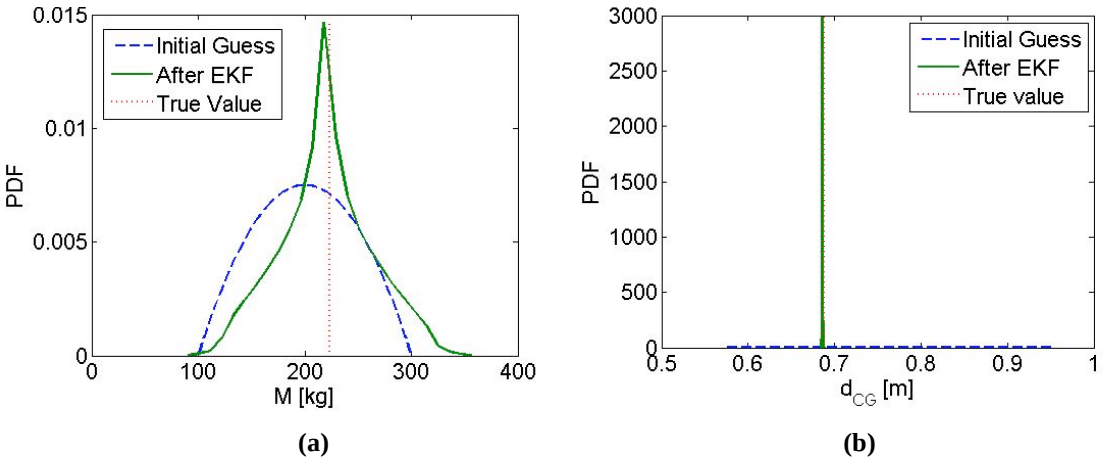

Figure 17. EKF estimation (whole set of data at once) for the linearized system at 1 Hz with 100 time points (noise = 1%); **Notes:** a) Mass in the form of PDF, b) Distance in the form of PDF

4. Summary and Conclusions

In this study, a new computational approach for parameter identification is proposed based on the application of polynomial chaos theory. An Extended Kalman Filter (EKF) is used to recalculate the polynomial chaos expansions for the uncertain states and the uncertain parameters. Two variations of the approach are used: the one-time-step-at-a-time EKF approach, in which the Kalman filter formula is used at each time step in order to update the polynomial chaos expressions of the uncertain states and the uncertain parameters, and the whole-set-of-data-at-once EKF approach, which consists of applying the filter formula only once, on a vector containing all the observations until the last time sample. For linear systems with Gaussian assumptions, the two approaches are equivalent in theory, but not necessarily in practice due to numerical issues.

Parameter estimation was performed on a nonlinear four degree of freedom roll plane model of a vehicle, in which an uncertain mass with an uncertain position is added on the roll bar. Uncertainties on the values of the added mass and its position were assumed to have a Beta (2, 2) distribution. The value of the mass and its position were estimated from periodic observations of the displacements and velocities across the suspensions, generated with synthetic measurements obtained from a reference simulation with the reference values of the uncertain parameters and with added noise. Two different inputs were used: a speed bump with the vehicle rolling over it at a constant speed, and a 1-Hz sinusoidal roll input.

The proposed method has several advantages. The polynomial chaos approach has been shown to be considerably more efficient than Monte Carlo methods in the simulation of systems with a small number of uncertain parameters, and the EKF approach gives more information about the parameters of interest than a simple estimated value: the estimation comes in the form of a probability density function. The one-time-step-at-a-time EKF approach usually yielded good estimations with a sampling rate of 0.3 s, with PDFs including the true values of the parameters. However, when using measurements with a sampling rate of 0.03 s, the one-time-step-at-a-time EKF approach yielded incoherent results. The erratic behavior of the PDF in function of the time was indicating that the results could not be trusted. The problem is that the EKF can diverge when using a high sampling frequency, which might prevent the use of enough data to obtain good results when a low sampling frequency is necessary. When applying the polynomial chaos theory to the Extended Kalman Filter, numerical errors can accumulate even faster than in the general case due to the truncation in the polynomial chaos expansions, which is illustrated on a simple example in Appendix. In most cases, the whole-set-of-data-at-once EKF approach yielded accurate results, with standard deviations of the estimates usually much smaller than the ones obtained with the one-time-step-at-a-time EKF approach. The whole-set-of-data-at-once EKF approach usually also worked well with a sampling rate of 0.03 s as well, but not always: the case in which the uncertain mass was estimated using the 1 Hz input showed that it could sometimes yield results that should not be trusted since the PDF contains values outside the range of possible values, even though the corresponding probabilities are low. Therefore, using different sampling rates in order to verify the coherence of the results is strongly recommended.

Since comparing the results to a different approach is also strongly recommended, future work will compare the results obtained with EKF approach to results obtained with a polynomial chaos – based Bayesian approach. We also plan to apply the proposed techniques to identify parameters of a real mechanical system for which laboratory measurements are available.

Acknowledgements

This research was supported in part by NASA Langley through the Virginia Institute for Performance Engineering and Research award. The authors are grateful to Dr. Mehdi Ahmadian, Dr. Steve Southward, Dr. John Ferris, and Mr. Carvel Holton for many fruitful discussions on this topic.

References

Blanchard, E., Sandu, C., and Sandu, A. (2007a), "A Polynomial-Chaos-based Bayesian Approach for Estimating Uncertain Parameters of Mechanical Systems", Proceedings of the ASME 2007 International Design Engineering Technical Conferences & Computers and Information in Engineering Conference IDETC/CIE 2007, 9th International Conference on Advanced Vehicle and Tire Technologies (AVTT), Las Vegas, Nevada, September.

Blanchard, E., Sandu, A., and Sandu, C. (2007b), "Parameter Estimation Method Using an Extended Kalman Filter", Proceedings of the Joint North America, Asia-Pacific ISTVS Conference and Annual Meeting of Japanese Society for Terramechanics, Fairbanks, Alaska, June.

Blanchard, E., Sandu, A., and Sandu, C. (2007c), "A Polynomial Chaos Based Bayesian Approach for Estimating Uncertain Parameters of Mechanical Systems – Part I: Theoretical Approach", Technical Report TR-07-38, Computer Science Department of Virginia Tech.

Blanchard, E., Sandu, A., and Sandu, C. (2007d), "A Polynomial Chaos Based Bayesian Approach for Estimating Uncertain Parameters of Mechanical Systems – Part II: Applications to Vehicle Systems" , Technical Report TR-07-39, Computer Science Department of Virginia Tech.

Cohn, S. E. (1997), "An Introduction to Estimation Theory", *Journal of the Meteorological Society of Japan*, Vol. 75 (B), pp. 257-288.

Evensen, G. (1992), "Using the Extended Kalman Filter with a Multi-layer Quasi-geostrophic Ocean Model", *Journal of Geophysical Research*, Vol 97 (C11), pp. 17905-17924.

Evensen, G. (1993), "Open Boundary Conditions for the Extended Kalman Filter with a Quasi-geostrophic Mode", *Journal of Geophysical Research*, Vol. 98 (C19) , pp.16529-16546.

Fisher, M. (2002), *Assimilation Techniques(5): Approximate Kalman Filters and singular vectors*

Ghanem, R.G., and Spanos, P.D. (2003), *Stochastic Finite Elements*, Dover Publications Inc, Mineola, NY.

Ghanem, R.G., and Spanos, P.D. (1990), "Polynomial Chaos in Stochastic Finite Element", *Journal of Applied Mechanics*, Vol. 57, pp. 197-202.

Ghanem, R.G., and Spanos, P.D. (1991), "Spectral Stochastic Finite-Element Formulation for Reliability Analysis", *ASCE Journal of Engineering Mechanics*, Vol. 117 No. 10, pp. 2351-2372.

Ghanem, R.G., and Spanos, P.D. (1993), "A Stochastic Galerkin Expansion for Nonlinear Random Vibration Analysis", *Probabilistic Engineering Mechanics*, Vol. 8 No. 3, pp. 255-264.

Halton, J. H., Smith, G. B. (1964), "Radical-inverse quasi-random point sequence", *Communications of the ACM*, Vol. 7 No. 12, pp. 701–702.

Hammersley, J. M. (1960) "Monte Carlo Methods for Solving Multivariables Problems", *Annals of the New York Academy of Sciences*, Vol. 86, pp. 844–874.

Kalman, R. E. (1960), "A New Approach to Linear Filtering and Prediction Problems", *Transaction of the ASME-Journal of Basic Engineering*, pp. 35-45.

Li, L., Sandu, C., and Sandu, A. (2005), "Modeling and Simulation of a Full Vehicle with Parametric and External Uncertainties", Proceedings of the 2005 ASME Int. Mechanical Engineering Congress and Exposition, 7th VDC Annual Symposium on "Advanced Vehicle Technologies", Session 4: Advances in Vehicle Systems Modeling and Simulation, Paper number IMECE2005-82101, Orlando, FL, November.

Sandu, A., Sandu, C., and Ahmadian, M. (2006a), "Modeling Multibody Dynamic Systems with Uncertainties. Part I: Theoretical and Computational Aspects", *Multibody System Dynamics*, Publisher: Springer Netherlands, ISSN: 1384-5640 (Paper) 1573-272X (Online), DOI 10.1007/s11044-006-9007-5, pp. 1-23 (23), June 29, 2006.

Sandu, C., Sandu, A., and Ahmadian, M. (2006b), "Modeling Multibody Dynamic Systems with Uncertainties. Part II: Numerical Applications", *Multibody System Dynamics*, Publisher: Springer Netherlands, ISSN: 1384-5640 (Paper) 1573-272X (Online), DOI: 10.1007/s11044-006-9008-4, Vol. 15, No. 3, pp. 241 - 262 (22), April 2006.

Sandu, C., Sandu, A., Chan, B.J., and Ahmadian, M. (2004), "Treating Uncertainties in Multibody Dynamic Systems using a Polynomial Chaos Spectral Decomposition", Proceedings of the ASME IMECE 2004, 6th Annual Symposium on "Advanced Vehicle Technology", Paper number IMECE2004-60482, Anaheim, CA, November.

Sandu, C., Sandu, A., Chan, B.J., and Ahmadian, M. (2005), "Treatment of Constrained Multibody Dynamic Systems with Uncertainties", Proceedings of the SAE Congress 2005, Paper number 2005-01-0936, Detroit, MI, April.

Sandu, C., Sandu, A., and Li, L. (2006c), "Stochastic Modeling of Terrain Profiles and Soil Parameters", *SAE 2005 Transactions Journal of Commercial Vehicles*, Vol. 114 No. 2, pp. 211-220.

Sohns, B., Allison, J., Fathy, H.K., Stein, J.L. (2006), "Efficient Parameterization of Large-Scale Dynamic Models Through the Use of Activity Analysis", Proceedings of the ASME IMECE 2006, Chicago, Illinois, November.

Xiu, D., Lucor, D., Su, C.H., and Karniadakis, G.E. (2002), "Stochastic Modeling of Flow-Structure Interactions using Generalized Polynomial Chaos", *Journal of Fluids Engineering*, Vol. 124, pp. 51-59.

Xiu, D., and Karniadakis, G.E. (2002a), "The Wiener-Askey Polynomial Chaos for Stochastic Differential Equations", *Journal on Scientific Computing*, Vol. 24 No. 2, pp. 619-644.

Xiu, D., and Karniadakis, G.E. (2002b), "Modeling Uncertainty in Steady-state Diffusion problems via Generalized Polynomial Chaos", *Computer Methods in Applied Mechanics and Engineering*, Vol. 191, pp. 4927-4928.

Xiu, D., and Karniadakis, G.E. (2003), "Modeling Uncertainty in Flow Simulations via Generalized Polynomial Chaos", *Journal of Computational Physics*, Vol. 187, pp. 137-167.

Zhang, D., Lu, Z. (2004), "An efficient, high-order perturbation approach for flow in random porous media via Karhunen–Loeve and polynomial expansions", *Journal of Computational Physics*, Vol. 194 No. 2, pp. 773–794.

List of Figures

List of Tables

Appendix: EKF – Error Analysis

The objective of this analysis is to show that the truncations in the polynomial chaos expansions can prevent the convergence of the covariance of the assimilated state and that the error can decrease with the length of the time step when there is no model error (which was the case for this study: the EKF approach assumes that the equations of motion of the system are perfectly known). This analysis will also show that when model errors are present, a nonzero optimal time step can exist.

A1. Framework

Consider the scalar system $y' = a\,y$ with $a < 0$, which is considered to be the true system, with initial condition y_0^{true}. It has a well-known analytical solution: $y(t) = y_0\, e^{a\,t}$. After k time steps Δt which are assumed to be constant, the "true" value of the state variable y is:

$$y_k^{true} = e^{a\,\Delta t}\; y_{k-1}^{true} = e^{k\,a\,\Delta t}\; y_0^{true} \tag{A1.1}$$

Using the notation $b = e^{a\,\Delta t}$, it can also be written as:

$$y_k^{true} = b\; y_{k-1}^{true} = b^k\; y_0^{true} \tag{A1.2}$$

Let's notice that $a < 0$ is equivalent to $0 < b < 1$.

A perturbed model will be used:

$$y' = a\,y + \varepsilon\;,\quad y(0) = y_0^a \tag{A1.3}$$

It is also assumed that the error model $\varepsilon(t)$ is independent Gaussian with mean B (B is the bias) and covariance Q. For the sake of simplicity, it will also be assumed that $\varepsilon(t)$ is fixed during each time interval Δt, i.e., that it takes the fixed value ε_{k+1} between time t_k and t_{k+1}.

A2. Recurrence relationships – Error and Covariance

The state y is propagated using the model equations:

$$y_{k+1}^f = e^{a\,\Delta t}\, y_k^a + \varepsilon_{k+1}\left(\frac{e^{a\,\Delta t} - 1}{a}\right) \tag{A2.1}$$

where the superscript *f* stands for forecast and the superscript *a* stands for assimilated.

The assimilated state at step k, y_k^a, is given by:

$$y_k^a = (1 - K_k)\, y_k^f + K_k\; y_k^{obs}\;, \tag{A2.3}$$

where K_k is the Kalman gain at step k, given by

$$K_k = P_k^f\, H_k{}^T \left(R_k + H_k\, P_k^f\, H_k{}^T\right)^{-1} \tag{A2.3}$$

In the 1-dimentional case, each matrix becomes a scalar. For our case, we will assume that all the R_k's can be replaced by R, which means that the noise level associated with the measurements is assumed to be constant. We will also assume that $H_k = 1$, i.e., we can directly measure y. Therefore, the Kalman gain at step k is

$$K_k = \frac{P_k^f}{R + P_k^f} \tag{A2.4}$$

and the assimilated state at step k, y_k^a, is given by:

$$y_k^a = \frac{R}{R + P_k^f} y_k^f + \frac{P_k^f}{R + P_k^f} y_k^{obs} \tag{A2.5}$$

Using the notation $c = \frac{e^{a\,\Delta t} - 1}{a} = \frac{b-1}{a}$, the model equation can be rewritten as

$$y_{k+1}^f = b\, y_k^a + c\, \varepsilon_{k+1} \tag{A2.6}$$

Let E_k^a be the error at step k after assimilation,

$$E_k^a = y_k^a - y_k^{true} \tag{A2.7}$$

Then, the "forecast" error at step $k+1$ (before assimilation) is given by:

$$E_{k+1}^f = b\, E_k^a + c\, \varepsilon_{k+1} \tag{A2.8}$$

Therefore,

$$< E_{k+1}^f > = b\ < E_k^a > + c\, B \tag{A2.9}$$

$$E_{k+1}^f - < E_{k+1}^f > = b\left(E_k^a - < E_k^a > \right) + c\,(\varepsilon_k - B) \tag{A2.10}$$

$$\left\langle \left(E_{k+1}^f - < E_{k+1}^f > \right)^2 \right\rangle = b^2 \left\langle \left(E_k^a - < E_k^a > \right)^2 \right\rangle + c^2 < \varepsilon_k - B >^2 + \underbrace{\left\langle b < \left(E_k^a - < E_k^a > \right), < \varepsilon_k - B > \right\rangle}_{= 0\ \ (uncorrelated)} \tag{A2.11}$$

which can also be written as

$$P_{k+1}^f = b^2\, P_k^a + c^2\, Q \tag{A2.12}$$

where P_{k+1}^f is the forecast variance a step $k+1$.

The objective of this analysis is to study the effect of the polynomial chaos approximation. Therefore, a term μ due to the truncation in the polynomial chaos expansion will be added to the forecast covariance:

$$P_{k+1}^f = b^2\, P_k^a + c^2\, Q + \mu \tag{A2.13}$$

For the sake of simplicity, μ will be assumed to be a constant.

Using the notation $\zeta = c^2\, Q + \mu$ yields

$$P_{k+1}^f = b^2\, P_k^a + \zeta \tag{A2.14}$$

Let's note that ζ is a constant for a constant time interval Δt. An independent Gaussian noise η with mean zero and covariance R to the observations:

$$y_{k+1}^{obs} = y_{k+1}^{true} + \eta_{k+1} = b\, y_k^{true} + \eta_{k+1} = b^{k+1}\, y_0^{true} + \eta_{k+1} \tag{A2.15}$$

The assimilated state at step $k+1$, y_{k+1}^a, is given by

$$y_{k+1}^a = (1 - K_{k+1})\, y_{k+1}^f + K_{k+1}\, y_{k+1}^{obs} \tag{A2.16}$$

Using the notation $E_k = E_k^a$ (i.e., E_k is the error after assimilation at step k), the error after assimilation at step $k+1$ is:

$$E_{k+1} = y_{k+1}^a - y_{k+1}^{true} = y_{k+1}^a - b\, y_k^{true} \tag{A2.17}$$

$$E_{k+1} = (1-K_{k+1})\, b\, y_k^a + K_{k+1}\, b\, y_k^{true} - b\, y_k^{true} + (1-K_{k+1})\, c\, \varepsilon_{k+1} + K_{k+1}\, y_{k+1} \tag{A2.18}$$

$$E_{k+1} = (1-K_{k+1})\, b\, y_k^a - (1-K_{k+1})\, b\, y_k^{true} + (1-K_{k+1})\, c\, \varepsilon_{k+1} + K_{k+1}\, \eta_{k+1} \tag{A2.19}$$

$$E_{k+1} = (1-K_{k+1})\, b\, (y_k^a - y_k^{true}) + (1-K_{k+1})\, c\, \varepsilon_{k+1} + K_{k+1}\, \eta_{k+1} \tag{A2.20}$$

$$E_{k+1} = (1-K_{k+1})\, b\, E_k + (1-K_{k+1})\, c\, \varepsilon_{k+1} + K_{k+1}\, \eta_{k+1} \tag{A2.21}$$

For our 1-dimentional example the Kalman gain at step $k+1$ is

$$K_{k+1} = \frac{P_{k+1}^f}{R + P_{k+1}^f} \tag{A2.22}$$

which yields

$$E_{k+1} = \frac{R\, b\, E_k + R\, c\, \varepsilon_{k+1} + P_{k+1}^f\, \eta_{k+1}}{R + P_{k+1}^f} \tag{A2.23}$$

Replacing P_{k+1}^f by its expression given in equation (A2.14) yields:

$$E_{k+1} = \frac{R\, b\, E_k + R\, c\, \varepsilon_{k+1} + (b^2\, P_k^a + \zeta)\, \eta_{k+1}}{R + b^2\, P_k^a + \zeta} \tag{A2.24}$$

The assimilated covariance at step $k+1$, P_{k+1}^a, is given by:

$$P_{k+1}^a = P_{k+1}^f - K_{k+1}\, H_{k+1}\, P_{k+1}^f \tag{A2.25}$$

For our 1-dimentional case, it is assumed that $H_k = 1$, and K_{k+1} is given in equation (A2.22), which yields

$$P_{k+1}^a = \frac{R\, P_{k+1}^f}{R + P_{k+1}^f} \tag{A2.26}$$

Replacing P_{k+1}^f by it expression given in equation (A2.14) yields:

$$P_{k+1}^a = \frac{R\, (b^2\, P_k^a + \zeta)}{R + b^2\, P_k^a + \zeta} \tag{A2.27}$$

A3. Convergence of the covariance of the assimilated state

Using the recurrence for the error and the covariance after assimilation yields the following Jacobian matrix:

$$\begin{pmatrix} \frac{dE_{k+1}}{dE_k} & \frac{dE_{k+1}}{dP_k^a} \\ \frac{dP_{k+1}^a}{dE_k} & \frac{dP_{k+1}^a}{dP_k^a} \end{pmatrix} = \begin{pmatrix} \frac{b\,R}{b^2\,P_k^a + R + \zeta} & \frac{b^2\,R\,(-b\,E_{k+1} - c\,\varepsilon_{k+1} + \eta_{k+1})}{\left(b^2\,P_k^a + R + \zeta\right)^2} \\ 0 & \left(\frac{b\,R}{b^2\,P_k^a + R + \zeta}\right)^2 \end{pmatrix} \tag{A3.1}$$

which yields the conditions for linear stability:

$$-1 < \frac{b\,R}{b^2\,P_k^a + R + \zeta} < 1 \tag{A3.2}$$

which is equivalent to the following two conditions

$$\frac{b^2\,P_k^a + R + \zeta}{b\,R} > 1 \quad \text{or} \quad \frac{b^2\,P_k^a + R + \zeta}{b\,R} < -1 \tag{A3.3}$$

i.e..

$$\zeta > -b^2\,P_k^a + (b-1)\,R \quad \text{or} \quad \zeta < -b^2\,P_k^a - (b+1)\,R \tag{A3.4}$$

The second case, $\zeta < -b^2\,P_k^a - (b+1)\,R$, cannot result in the convergence of P_k^a because it is impossible to have $\zeta < -b^2\,P_{conv} - (b+1)\,R$ with $P_{conv} \geq 0$. This has been proved with Mathematica, as shown below.

```
P_conv = (-(1 - b^2) R - ζ + Sqrt[4 b^2 R ζ + ((1 - b^2) R + ζ)^2]) / (2 b^2) ;

Reduce[P_conv ≥ 0 && Q > 0 && R > 0 && 0 < b < 1 && ζ < -b^2 P_conv - (b + 1) R, ζ, Reals]

False
```

It means that the only case for which the covariance converges is when:

$$\zeta > -b^2\,P_k^a - (1-b)\,R \tag{A3.5}$$

or equivalently, when

$$\mu > -b^2\,P_k^a - (1-b)\,R - \left(\frac{1-b}{a}\right)^2 Q, \quad b = e^{a\,\Delta t} \tag{A3.6}$$

which also forces the following condition to be true

$$\zeta \geq 0 \text{ , i.e. } \mu \geq -\left(\frac{1-b}{a}\right)^2 Q \tag{A3.7}$$

which can be proved by using Mathematica, as shown below.

$$P_{conv} = \left(-\left(1-b^2\right) R - \xi + \sqrt{4\,b^2\,R\,\xi + \left(\left(1-b^2\right) R + \xi\right)^2}\right) \Big/ \left(2\,b^2\right) ;$$

$$\text{Reduce}\left[P_{conv} \geq 0 \;\&\&\; Q > 0 \;\&\&\; R > 0 \;\&\&\; 0 < b < 1 \;\&\&\; \xi > -b^2\,P_{conv} - (1-b)\,R,\; \xi,\; \text{Reals}\right]$$

$$R > 0 \;\&\&\; Q > 0 \;\&\&\; 0 < b < 1 \;\&\&\; \xi \geq 0$$

We have just showed that the convergence P_k^a, i.e., the convergence of the covariance of y_k^a, is affected by the truncations in the polynomial chaos expansions. Let's remind that $P_{k+1}^f = b^2\,P_k^a + \xi$. It means that overestimating the covariance is not a problem, but underestimating prevents the convergence of the covariance. It can be explained by looking at equation (A2.4) and seeing that a very large forecast covariance results in a Kalman gain close to 1, which means that the assimilated value of the state y will be very similar to the observation and the impact of the previous error will be gone, which can be seen by looking at equation (A2.16). When the forecast covariance is very small, the Kalman gain will be close to 0, and the assimilated value of the state y will be very similar to its forecast value, which means that the convergence of the covariance will be slow.

Let us find the value P_{conv} towards which the covariance P_k^a converges to when is converges. The assimilated covariance at step $k+1$, P_{k+1}^a, is given by:

$$P_{k+1}^a = P_{k+1}^f - K_{k+1}\,H_{k+1}\,P_{k+1}^f \tag{A3.8}$$

which yields

$$P_{k+1}^a = \frac{R\,(b^2\,P_k^a + \xi)}{R + b^2\,P_k^a + \xi} \tag{A3.9}$$

Therefore, if the covariance convergences, it converges to

$$P_{conv} = \frac{-(1-b^2)\,R - \xi + \sqrt{4\,b^2\,R\,\xi + ((1-b^2)\,R + \xi)^2}}{2\,b^2} \tag{A3.10}$$

A4. Error after the covariance of the assimilated state has converged

The recurrence relationship for the error after assimilation is:

$$E_{k+1} = \frac{R\,b\,E_k + R\,c\,\varepsilon_{k+1} + (b^2\,P_k^a + \xi)\,\eta_{k+1}}{R + b^2\,P_k^a + \xi} \tag{A4.1}$$

Therefore, after convergence, the recurrence relationship for the error after assimilation becomes:

$$E_{k+1} = \frac{R\,b\,E_k + R\,c\,\varepsilon_{k+1} + (b^2\,P_{conv} + \xi)\,\eta_{k+1}}{R + b^2\,P_{conv} + \xi} \tag{A4.2}$$

The EKF error recurrence after P_k^a convergences to P_{conv} becomes:

$$E_{k+1} = M\,E_k + \alpha\,\varepsilon_{k+1} + \beta\,\eta_{k+1} \tag{A4.3}$$

with

$$M = \frac{b\,R}{R + b^2\,P_{conv} + \xi}, \quad \alpha = \frac{c\,R}{R + b^2\,P_{conv} + \xi}, \quad \beta = \frac{(b^2\,P_{conv} + \xi)}{R + b^2\,P_{conv} + \xi} \tag{A4.4}$$

If we rename the steps so that the step $k = 0$ is the first step, the error E_N (N steps after P_k^a convergences to P_{conv}, after assimilation) can be written as:

$$E_N = M^N E_0 + \alpha \sum_{i=1}^{N-1} M^i \varepsilon_{N-i} + \beta \sum_{i=1}^{N-1} M^i \eta_{N-i} \tag{A4.5}$$

The fact that E_0 is the error at a new step and therefore has a different value does not matter when studying the convergence of equation (A4.5) since $M^N = \left(\frac{b R}{R + b^2 P_{conv} + \zeta} \right)^N \to 0$ as $N \to \infty$.

Therefore, for large values of N, i.e., long after the covariance has converged.

$$E_N = \alpha \sum_{i=1}^{N-1} M^i \varepsilon_{N-i} + \beta \sum_{i=1}^{N-1} M^i \eta_{N-i} \tag{A4.6}$$

For ε_i's independent Gaussian with mean B and covariance Q, the term $\alpha \sum_{i=1}^{N-1} M^i \varepsilon_{N-i}$ is Gaussian with mean $\alpha \sum_{i=1}^{N-1} M^i B = B \alpha \frac{1 - M^N}{1 - M} \approx \frac{B \alpha}{1 - M}$ and covariance $\alpha^2 Q \sum_{i=1}^{N-1} M^{2i} \approx \frac{\alpha^2 Q}{1 - M^2}$. When $N \to \infty$, the term $\alpha \sum_{i=1}^{N-1} M^i \varepsilon_{N-i}$ is Gaussian with mean $\frac{B \alpha}{1 - M}$ and covariance $\frac{\alpha^2 Q}{1 - M^2}$. Similarly, for η_i's independent Gaussian with mean zero and covariance R, $\beta \sum_{i=1}^{N-1} M^i \eta_{N-i}$ is Gaussian with mean zero and covariance $\beta^2 R \sum_{i=1}^{N-1} M^{2i} = \beta^2 R \frac{1 - M^{2N}}{1 - M^2}$. When $N \to \infty$, the term $\beta \sum_{i=1}^{N-1} M^i \eta_{N-i}$ is Gaussian with mean zero and covariance $\frac{\beta^2 R}{1 - M^2}$.

Since the error model and the measurement noise are not correlated, the covariance of E_N is the sum of the covariance of $\alpha \sum_{i=1}^{N-1} M^i \varepsilon_{N-i}$ and the covariance of $\beta \sum_{i=1}^{N-1} M^i \eta_{N-i}$. The mean value of E_N is also the sum of the mean values of the different terms in the sum. Therefore, when $N \to \infty$, the mean value of E_N is $\frac{B \alpha}{1 - M}$ and the covariance of E_N is $\frac{\alpha^2 Q + \beta^2 R}{1 - M^2}$, with α, β and M defined in equation (A4.4). In Appendix A6, these are expressed in terms of b, R, Q, B, a and μ, which is implicitly in terms of Δt, R, Q, B, a and μ since $b = e^{a \Delta t}$.

Summary - Error after the covariance of the assimilated state has converged:

For large values of N, the error after assimilation N steps after the covariance has converged, E_N, has a mean value $\frac{B \alpha}{1 - M}$ with a covariance $\frac{\alpha^2 Q + \beta^2 R}{1 - M^2}$ with:

$$M = \frac{b R}{R + b^2 P_{conv} + \zeta}, \quad \alpha = \frac{c R}{R + b^2 P_{conv} + \zeta}, \quad \beta = \frac{(b^2 P_{conv} + \zeta)}{R + b^2 P_{conv} + \zeta}$$

$$P_{conv} = \frac{-(1 - b^2) R - \zeta + \sqrt{4 b^2 R \zeta + ((1 - b^2) R + \zeta)^2}}{2 b^2}, \quad \zeta = c^2 Q + \mu, \quad c = \left(\frac{b - 1}{a} \right), \quad b = e^{a \Delta t}$$

A5. Possible optimal time steps

Finding a simple analytical expression of the time step Δt that minimizes the expression of the mean or the covariance of E_N, or even simply the covariance of $\alpha \sum_{i=1}^{N-1} M^i \varepsilon_{N-i}$ or the covariance of $\beta \sum_{i=1}^{N-1} M^i \eta_{N-i}$, is not possible in the general case, as illustrated in Appendix A6. With Mathematica, we cannot find analytical expressions for the b's that set the derivatives of these expressions with respect to b to 0, which would yield an optimal time step $\Delta t_{opt} = \frac{1}{a} Log_n(b_{opt})$ when the second derivative with respect to b is positive.

However, in the case where there is no model error ($B = 0$, $Q = 0$), it can be shown analytically that the derivative of the total covariance of E_N (which is also equal to the covariance of $\beta \sum_{i=1}^{N-1} M^i \eta_{N-i}$ in that case) with respect to b is positive, which means that the covariance increases with $b = e^{a\Delta t}$, so decreases with Δt since $a < 0$. The derivation is shown in Appendix A5 with Mathematica. A numerical example is shown in Figure A1, where the covariance of E_N is plotted for different time steps, assuming a perfect model ($B = 0$, $Q = 0$). The scalar system used for this example is $y' = -y$, i.e., $a = -1$.

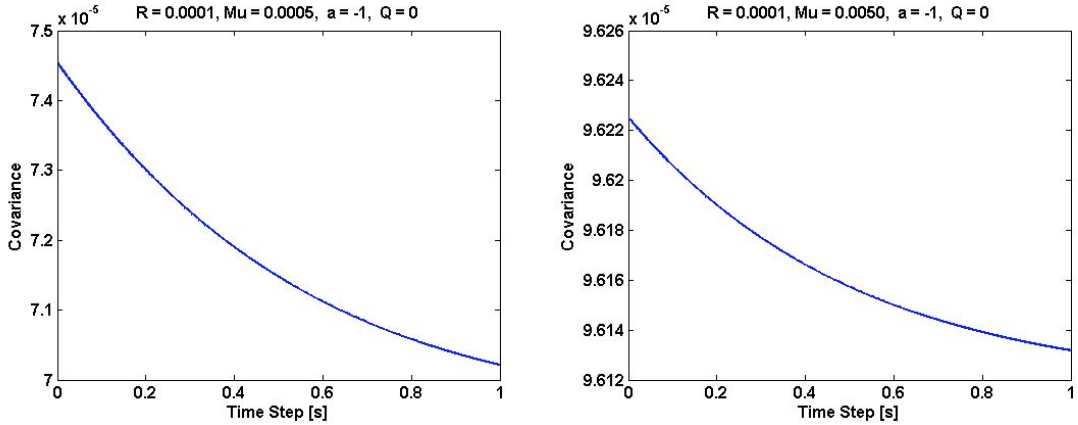

(a) **(b)**

Figure A1. Covariance after convergence of the covariance with no model error (Q = 0, B = 0);
(a) R = 0.0001, Mu = 0.0005, a = -1, ; (b) R = 0.0001, Mu = 0.0050, a = -1

Therefore, when there is no model error, it can be shown analytically that the error decreases with Δt, which means a larger Δt results in a smaller error. Figure 8 showed the absolute error for our two estimated parameters, i.e., $\left| \xi_{1,est} - \xi_{1,ref} \right|$ and $\left| \xi_{2,est} - \xi_{2,ref} \right|$, with the nonlinear half-car model for the speed bump with respect to the different corresponding time steps. It is reproduced in Figure A2. There was no model error and a Gaussian measurement noise of mean 0 and variance 1% was added to the observation. It could be observed that for this case study with a perfect model, the error gets worse for small time steps Δt. The fact that the error can get larger as the time step is increase too much was due to the fact that with very few observations, the covariance had not converged yet. For instance, with a time step of 1.5 seconds, only two significant measurements were available. The error for the case study $y' = -y$, which was plotted in Figure A1, was calculated assuming the covariance had already converged.

With numerical examples, it can be shown that a nonzero optimal time step can exist when $Q \neq 0$, i.e., when there is a model error. Figure A3 shows an example where the model error has no bias, i.e., with $B = 0$. The covariance of

E_N is the sum of the covariance of $\alpha \sum_{i=1}^{N-1} M^i \varepsilon_{N-i}$, shown in Figure A3(a) and the covariance of $\beta \sum_{i=1}^{N-1} M^i \eta_{N-i}$, shown in Figure A3(b). For the example shown in Figure A3, the covariance of E_N is approximately equal to the covariance of $\beta \sum_{i=1}^{N-1} M^i \eta_{N-i}$, so it is not displayed in Figure A3 since it would impossible to notice any difference with the covariance of E_N. For the example shown in Figure A3, there is a nonzero optimal time step that minimizes the covariance of the estimation error. Even though the covariance of $\alpha \sum_{i=1}^{N-1} M^i \varepsilon_{N-i}$ is very small compared with the covariance $\beta \sum_{i=1}^{N-1} M^i \eta_{N-i}$, the fact that $Q \neq 0$ completely changes the shape of the covariance $\beta \sum_{i=1}^{N-1} M^i \eta_{N-i}$, and therefore the shape of the covariance of E_N: there is a nonzero optimal time step that minimizes the covariance of the estimation error (0.015 s in this case).

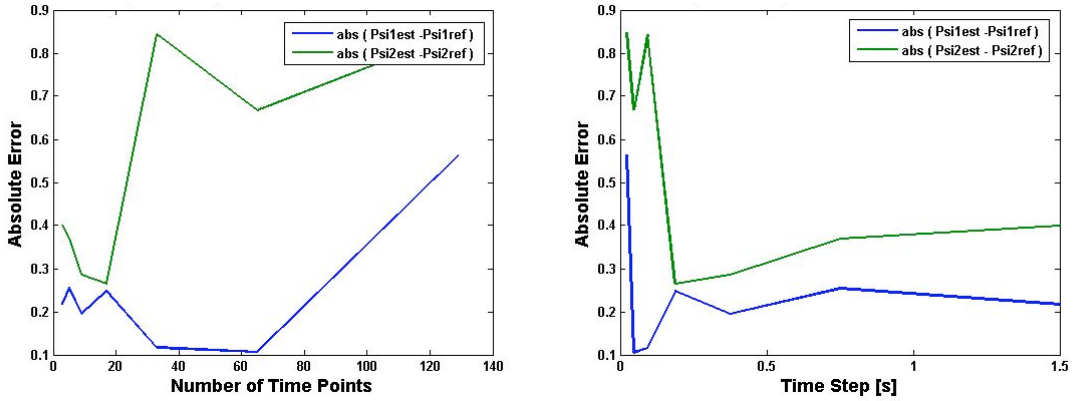

(a) **(b)**

Figure A2. Absolute Error for the Estimated Parameters ξ_1 and ξ_2 with the Nonlinear Half-Car Model for the Speed Bump with Respect to: (a) the Number of Time Points; (b) the Length of the Time Step

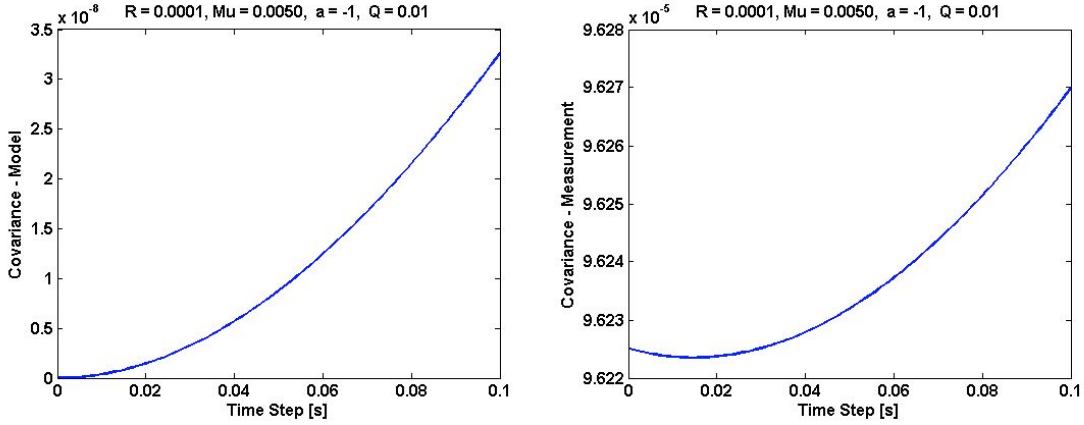

(a) **(b)**

Figure A3. Covariance of E_N after convergence for R = 0.0001, Mu = 0.0050, a = -1, Q = 0.01, B = 0 (i.e., model error, but with no bias);

(a) Covariance due to Model Errors; (b) Covariance due to Measurement Noise

Figure A4 shows an example where the model error has a bias, i.e., with $B \neq 0$. With a large bias, it can be observed that the error increases with the length of the time step.

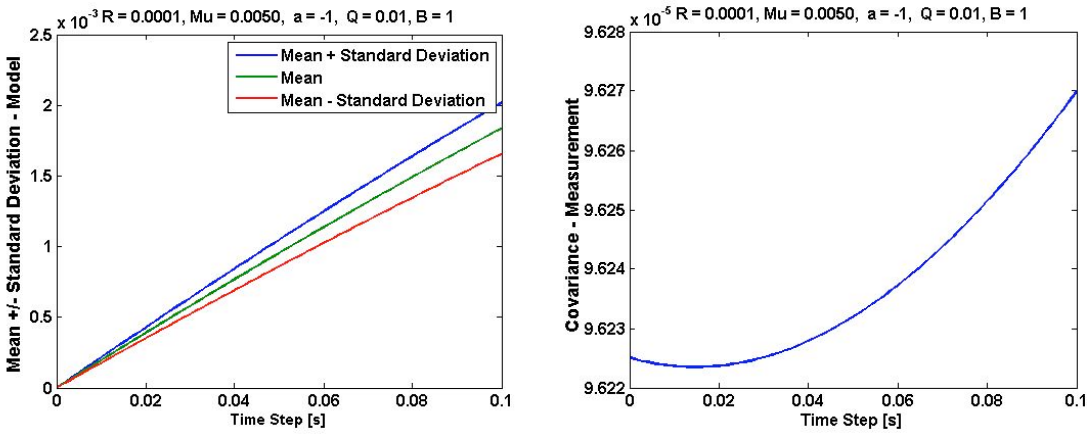

(a) **(b)**

Figure A4. Error for R = 0.0001, Mu = 0.0050, a = -1, Q = 0.01 B = 1; (i.e., model error, but with bias)

(a) Error due to Model Errors; (b) Covariance of Error due to Measurement Noise

A6. Detailed expressions of the mean errors and the covariances - Possible optimal time steps

The mean of E_N, which is also the mean of $\alpha \sum_{i=1}^{N-1} M^i \varepsilon_{N-i}$ is:

$$\text{MeanModel} = \frac{2\,B\,c\,R}{(-1+b)^2 R + \zeta + \sqrt{4\,b^2 R\,\zeta + (R - b^2 R + \zeta)^2}}$$

The covariance of $\alpha \sum_{i=1}^{N-1} M^i \varepsilon_{N-i}$ is:

$$\text{CovModel} = \frac{2\,c^2\,Q\,R^2}{(-1+b^2)^2 R^2 + \zeta\left(\zeta + \sqrt{(-1+b^2)^2 R^2 + 2\,(1+b^2)\,R\,\zeta + \zeta^2}\right) + (1+b^2)\,R\left(2\,\zeta + \sqrt{(-1+b^2)^2 R^2 + 2\,(1+b^2)\,R\,\zeta + \zeta^2}\right)}$$

The covariance of $\beta \sum_{i=1}^{N-1} M^i \eta_{N-i}$ is:

$$\text{CovMeas} = \frac{R\left(-R + b^2 R + \zeta + \sqrt{4\,b^2 R\,\zeta + (R - b^2 R + \zeta)^2}\right)^2}{2\left((-1+b^2)^2 R^2 + \zeta\left(\zeta + \sqrt{(-1+b^2)^2 R^2 + 2\,(1+b^2)\,R\,\zeta + \zeta^2}\right) + (1+b^2)\,R\left(2\,\zeta + \sqrt{(-1+b^2)^2 R^2 + 2\,(1+b^2)\,R\,\zeta + \zeta^2}\right)\right)}$$

The covariance of E_N is:

$$\text{CovTotal} = \frac{R\left(R\left(2\,c^2 Q + (-1+b^2)^2 R + 2\,b^2\,\zeta\right) + \zeta^2 - R\sqrt{4\,b^2 R\,\zeta + (R - b^2 R + \zeta)^2} + b^2 R\sqrt{4\,b^2 R\,\zeta + (R - b^2 R + \zeta)^2} + \zeta\sqrt{4\,b^2 R\,\zeta + (R - b^2 R + \zeta)^2}\right)}{(-1+b^2)^2 R^2 + \zeta\left(\zeta + \sqrt{(-1+b^2)^2 R^2 + 2\,(1+b^2)\,R\,\zeta + \zeta^2}\right) + (1+b^2)\,R\left(2\,\zeta + \sqrt{(-1+b^2)^2 R^2 + 2\,(1+b^2)\,R\,\zeta + \zeta^2}\right)}$$

In order to study the error and the covariances vs. the time step Δt , we need to replace c by $\left(\frac{b-1}{a}\right)$ and ζ by $\mu+\left(\frac{b-1}{a}\right)^2 Q$ in order to have only one variable that depends on Δt: $b = e^{a\,\Delta t}$.

Then we can take the derivative of the error and the covariances vs. $b = e^{a\,\Delta t}$ and try to find an optimal value of b_{opt} minimizing the expression we're trying to minimize by finding a b_{opt} resulting in the derivative equal to zero and by checking that the second derivative is positive at that point.

If an optimal time step exists, it will be $\Delta t_{opt} = \frac{1}{a} Log_n(b_{opt})$

Replacing c by $\left(\frac{b-1}{a}\right)$ and ζ by $\mu+\left(\frac{b-1}{a}\right)^2 Q$ yields the following expressions:

$$\text{MeanModel} = \frac{2\,(-1+b)\,B\,R}{a\left(\frac{(-1+b)^2 Q}{a^2} + (-1+b)^2 R + \mu + \sqrt{4\,b^2 R\left(\frac{(-1+b)^2 Q}{a^2}+\mu\right) + \left(\frac{(-1+b)^2 Q}{a^2} + R - b^2 R + \mu\right)^2}\right)}$$

$$\text{CovModel} = \frac{2\,(-1+b)^2 Q R^2}{a^2\left(\left(-1+b^2\right)^2 R^2 + \left(\frac{(-1+b)^2 Q}{a^2}+\mu\right)\left(\frac{(-1+b)^2 Q}{a^2}+\mu+\sqrt{\left(-1+b^2\right)^2 R^2 + 2\left(1+b^2\right) R\left(\frac{(-1+b)^2 Q}{a^2}+\mu\right) + \left(\frac{(-1+b)^2 Q}{a^2}+\mu\right)^2}\right) + \left(1+b^2\right) R\left(2\left(\frac{(-1+b)^2 Q}{a^2}+\mu\right)+\sqrt{\left(-1+b^2\right)^2 R^2 + 2\left(1+b^2\right) R\left(\frac{(-1+b)^2 Q}{a^2}+\mu\right) + \left(\frac{(-1+b)^2 Q}{a^2}+\mu\right)^2}\right)\right)}$$

$$\text{CovMeas} = \frac{R\left(\frac{(-1+b)^2 Q}{a^2} - R + b^2 R + \mu + \sqrt{4\,b^2 R\left(\frac{(-1+b)^2 Q}{a^2}+\mu\right) + \left(\frac{(-1+b)^2 Q}{a^2} + R - b^2 R + \mu\right)^2}\right)^2}{2\left(\left(-1+b^2\right)^2 R^2 + \left(\frac{(-1+b)^2 Q}{a^2}+\mu\right)\left(\frac{(-1+b)^2 Q}{a^2}+\mu+\sqrt{\left(-1+b^2\right)^2 R^2 + 2\left(1+b^2\right) R\left(\frac{(-1+b)^2 Q}{a^2}+\mu\right) + \left(\frac{(-1+b)^2 Q}{a^2}+\mu\right)^2}\right) + \left(1+b^2\right) R\left(2\left(\frac{(-1+b)^2 Q}{a^2}+\mu\right)+\sqrt{\left(-1+b^2\right)^2 R^2 + 2\left(1+b^2\right) R\left(\frac{(-1+b)^2 Q}{a^2}+\mu\right) + \left(\frac{(-1+b)^2 Q}{a^2}+\mu\right)^2}\right)\right)}$$

$$\text{CovTotal} = \frac{R\left(\frac{4\,(-1+b)^2 Q R}{a^2} + \left(\frac{(-1+b)^2 Q}{a^2} - R + b^2 R + \mu + \sqrt{4\,b^2 R\left(\frac{(-1+b)^2 Q}{a^2}+\mu\right) + \left(\frac{(-1+b)^2 Q}{a^2} + R - b^2 R + \mu\right)^2}\right)^2\right)}{2\left(\left(-1+b^2\right)^2 R^2 + \left(\frac{(-1+b)^2 Q}{a^2}+\mu\right)\left(\frac{(-1+b)^2 Q}{a^2}+\mu+\sqrt{4\,b^2 R\left(\frac{(-1+b)^2 Q}{a^2}+\mu\right) + \left(\frac{(-1+b)^2 Q}{a^2} + R - b^2 R + \mu\right)^2}\right) + \left(1+b^2\right) R\left(2\left(\frac{(-1+b)^2 Q}{a^2}+\mu\right)+\sqrt{4\,b^2 R\left(\frac{(-1+b)^2 Q}{a^2}+\mu\right) + \left(\frac{(-1+b)^2 Q}{a^2} + R - b^2 R + \mu\right)^2}\right)\right)}$$

In the general case, we cannot find analytical expressions for the b's that set the derivatives of these expressions to 0, even though we can show an optimal time step $\Delta t_{opt} = \frac{1}{a} Log_n(b_{opt})$ can exist with numerical examples. For instance, if we're trying to set the derivative of the mean of E_N to 0, which is the simplest case, we obtain:

```
Solve[D[MeanModel, b] == 0, b]
```

$$\{\{b \to \text{Root}[Q^3 + 2a^2Q^2R + a^4QR^2 + a^2Q^2\mu - a^6R^2\mu - a^4Q\mu^2 - 2a^6R\mu^2 - a^6\mu^3 + Q(-6Q^2 - 12a^2QR - 6a^4R^2 - 4a^2Q\mu - 4a^4R\mu + 2a^4\mu^2)\#1 + (15Q^3 + 30a^2Q^2R + 15a^4QR^2 + 6a^2Q^2\mu + 12a^4QR\mu + 6a^6R^2\mu - a^4Q\mu^2 - 2a^6R\mu^2)\#1^2 + (-20Q^3 - 40a^2Q^2R - 20a^4QR^2 - 4a^2Q^2\mu - 12a^4QR\mu - 8a^6R^2\mu)\#1^3 + (15Q^3 + 30a^2Q^2R + 15a^4QR^2 + a^2Q^2\mu + 4a^4QR\mu + 3a^6R^2\mu)\#1^4 + Q(-6Q^2 - 12a^2QR - 6a^4R^2)\#1^5 + Q(Q^2 + 2a^2QR + a^4R^2)\#1^6 \&, 1]\},$$
$$\{b \to \text{Root}[Q^3 + 2a^2Q^2R + a^4QR^2 + a^2Q^2\mu - a^6R^2\mu - a^4Q\mu^2 - 2a^6R\mu^2 - a^6\mu^3 + Q(-6Q^2 - 12a^2QR - 6a^4R^2 - 4a^2Q\mu - 4a^4R\mu + 2a^4\mu^2)\#1 + (15Q^3 + 30a^2Q^2R + 15a^4QR^2 + 6a^2Q^2\mu + 12a^4QR\mu + 6a^6R^2\mu - a^4Q\mu^2 - 2a^6R\mu^2)\#1^2 + (-20Q^3 - 40a^2Q^2R - 20a^4QR^2 - 4a^2Q^2\mu - 12a^4QR\mu - 8a^6R^2\mu)\#1^3 + (15Q^3 + 30a^2Q^2R + 15a^4QR^2 + a^2Q^2\mu + 4a^4QR\mu + 3a^6R^2\mu)\#1^4 + Q(-6Q^2 - 12a^2QR - 6a^4R^2)\#1^5 + Q(Q^2 + 2a^2QR + a^4R^2)\#1^6 \&, 2]\},$$
$$\{b \to \text{Root}[Q^3 + 2a^2Q^2R + a^4QR^2 + a^2Q^2\mu - a^6R^2\mu - a^4Q\mu^2 - 2a^6R\mu^2 - a^6\mu^3 + Q(-6Q^2 - 12a^2QR - 6a^4R^2 - 4a^2Q\mu - 4a^4R\mu + 2a^4\mu^2)\#1 + (15Q^3 + 30a^2Q^2R + 15a^4QR^2 + 6a^2Q^2\mu + 12a^4QR\mu + 6a^6R^2\mu - a^4Q\mu^2 - 2a^6R\mu^2)\#1^2 + (-20Q^3 - 40a^2Q^2R - 20a^4QR^2 - 4a^2Q^2\mu - 12a^4QR\mu - 8a^6R^2\mu)\#1^3 + (15Q^3 + 30a^2Q^2R + 15a^4QR^2 + a^2Q^2\mu + 4a^4QR\mu + 3a^6R^2\mu)\#1^4 + Q(-6Q^2 - 12a^2QR - 6a^4R^2)\#1^5 + Q(Q^2 + 2a^2QR + a^4R^2)\#1^6 \&, 3]\},$$
$$\{b \to \text{Root}[Q^3 + 2a^2Q^2R + a^4QR^2 + a^2Q^2\mu - a^6R^2\mu - a^4Q\mu^2 - 2a^6R\mu^2 - a^6\mu^3 + Q(-6Q^2 - 12a^2QR - 6a^4R^2 - 4a^2Q\mu - 4a^4R\mu + 2a^4\mu^2)\#1 + (15Q^3 + 30a^2Q^2R + 15a^4QR^2 + 6a^2Q^2\mu + 12a^4QR\mu + 6a^6R^2\mu - a^4Q\mu^2 - 2a^6R\mu^2)\#1^2 + (-20Q^3 - 40a^2Q^2R - 20a^4QR^2 - 4a^2Q^2\mu - 12a^4QR\mu - 8a^6R^2\mu)\#1^3 + (15Q^3 + 30a^2Q^2R + 15a^4QR^2 + a^2Q^2\mu + 4a^4QR\mu + 3a^6R^2\mu)\#1^4 + Q(-6Q^2 - 12a^2QR - 6a^4R^2)\#1^5 + Q(Q^2 + 2a^2QR + a^4R^2)\#1^6 \&, 4]\},$$
$$\{b \to \text{Root}[Q^3 + 2a^2Q^2R + a^4QR^2 + a^2Q^2\mu - a^6R^2\mu - a^4Q\mu^2 - 2a^6R\mu^2 - a^6\mu^3 + Q(-6Q^2 - 12a^2QR - 6a^4R^2 - 4a^2Q\mu - 4a^4R\mu + 2a^4\mu^2)\#1 + (15Q^3 + 30a^2Q^2R + 15a^4QR^2 + 6a^2Q^2\mu + 12a^4QR\mu + 6a^6R^2\mu - a^4Q\mu^2 - 2a^6R\mu^2)\#1^2 + (-20Q^3 - 40a^2Q^2R - 20a^4QR^2 - 4a^2Q^2\mu - 12a^4QR\mu - 8a^6R^2\mu)\#1^3 + (15Q^3 + 30a^2Q^2R + 15a^4QR^2 + a^2Q^2\mu + 4a^4QR\mu + 3a^6R^2\mu)\#1^4 + Q(-6Q^2 - 12a^2QR - 6a^4R^2)\#1^5 + Q(Q^2 + 2a^2QR + a^4R^2)\#1^6 \&, 5]\},$$
$$\{b \to \text{Root}[Q^3 + 2a^2Q^2R + a^4QR^2 + a^2Q^2\mu - a^6R^2\mu - a^4Q\mu^2 - 2a^6R\mu^2 - a^6\mu^3 + Q(-6Q^2 - 12a^2QR - 6a^4R^2 - 4a^2Q\mu - 4a^4R\mu + 2a^4\mu^2)\#1 + (15Q^3 + 30a^2Q^2R + 15a^4QR^2 + 6a^2Q^2\mu + 12a^4QR\mu + 6a^6R^2\mu - a^4Q\mu^2 - 2a^6R\mu^2)\#1^2 + (-20Q^3 - 40a^2Q^2R - 20a^4QR^2 - 4a^2Q^2\mu - 12a^4QR\mu - 8a^6R^2\mu)\#1^3 + (15Q^3 + 30a^2Q^2R + 15a^4QR^2 + a^2Q^2\mu + 4a^4QR\mu + 3a^6R^2\mu)\#1^4 + Q(-6Q^2 - 12a^2QR - 6a^4R^2)\#1^5 + Q(Q^2 + 2a^2QR + a^4R^2)\#1^6 \&, 6]\}\}$$

However, in the case where there is no model error ($Q = 0$, $B = 0$), it can be shown analytically that the derivative of the total covariance of E_N (which is also equal to the covariance of $\beta \sum_{i=1}^{N-1} M^i \eta_{N-i}$ in that case) with respect to b is positive, which means that the covariance increases with $b = e^{a\Delta t}$, so decreases with Δt since $a < 0$. The derivation with Mathematica is shown below. The expression calculated for the covariance of the error was defined only after P_k^a converges to P_{conv}, which means that equation (A3.7), i.e., $\zeta \geq 0$, has to be verified. In the case where there is no model error equation (A3.7) becomes equivalent to $\mu \geq 0$, which will therefore be used in the Mathematica code shown below.

```
CovTotalnoQ = Simplify[ CovTotal /. {Q→ 0}]
```

$$\frac{R\left(-R + b^2R + \mu + \sqrt{4b^2R\mu + \left(R - b^2R + \mu\right)^2}\right)^2}{2\left(\left(-1 + b^2\right)^2R^2 + \mu\left(\mu + \sqrt{4b^2R\mu + \left(R - b^2R + \mu\right)^2}\right) + \left(1 + b^2\right)R\left(2\mu + \sqrt{4b^2R\mu + \left(R - b^2R + \mu\right)^2}\right)\right)}$$

```
DerivCovTotalnoQ = D[CovTotalnoQ, b];
Reduce[DerivCovTotalnoQ < 0 && R > 0 && (μ ≥ 0  && (0 < b < 1)), Reals]
Reduce[DerivCovTotalnoQ == 0 && R > 0 && (μ ≥ 0  && (0 < b < 1)), Reals]
Reduce[DerivCovTotalnoQ > 0 && R > 0 && (μ ≥ 0  && (0 < b < 1)), Reals]
```

```
False
```

```
μ == 0 && 0 < b < 1 && R > 0
```

```
μ > 0 && 0 < b < 1 && R > 0
```